

# Deglacial and postglacial paleoseismological archives in mass-movement deposits of lakes of south-central Québec

## **Annie-Pier Trottier**

Centre d'études nordiques (CEN), Québec-Océan (QO) and Département de géographie, Université Laval, QC, Canada  
(514) 979-0474  
[annie-pier.trottier.1@laval.ca](mailto:annie-pier.trottier.1@laval.ca)

## **Patrick Lajeunesse**

Centre d'études nordiques (CEN), Québec-Océan (QO) and Département de géographie, Université Laval, QC, Canada  
[Patrick.Lajeunesse@ggr.ulaval.ca](mailto:Patrick.Lajeunesse@ggr.ulaval.ca)

## **Alexandre Normandeau<sup>1</sup>**

Centre d'études nordiques (CEN) and Département de géographie, Université Laval, QC, Canada

## **Antoine Gagnon-Poiré<sup>2</sup>**

Centre d'études nordiques (CEN) and Département de géographie, Université Laval, QC, Canada

---

<sup>1</sup> Geological Survey of Canada (Atlantic), Dartmouth, Nova Scotia, Canada  
[Alexandre.normandeau@canada.ca](mailto:Alexandre.normandeau@canada.ca)

<sup>2</sup> Institut national de recherche scientifique, Centre Eau Terre Environnement, Québec, Qc, Canada  
[Antoine.Gagnon-Poire@ete.inrs.ca](mailto:Antoine.Gagnon-Poire@ete.inrs.ca)

## 1 ABSTRACT

2 Investigation of seismic activity in eastern Canada is important for natural hazard  
3 management since two major active seismic zones with many historical records are located  
4 in the region: the Western Québec and the Charlevoix-Kamouraska seismic zones, with the  
5 latter being the most active in northeastern America. This paper describes and analyses a  
6 dataset of high-resolution swath bathymetric imagery, sub-bottom profiles and sediments  
7 cores collected in three lakes (Maskinongé, Aux-Sables and St-Joseph) located between two  
8 active seismic zones. The geomorphology observed on high-resolution swath bathymetric  
9 imagery, the acoustic sub-bottom profiles and the sediment analysis indicate that the lakes  
10 were disturbed by three phases of seismically-induced mass-movements since deglaciation :  
11 1) during the deglacial Champlain Sea transgression and the rapid initial glacio-isostatic  
12 rebound between ~13 and 10.5 ka cal. BP; 2) around 1180 AD; and 3) the well documented  
13 CKSZ 1663 AD  $M > 7$  historical earthquake. The second phase of earthquake events (1180  
14 AD) corresponds chronologically to a previously documented large-landslide in western  
15 Québec, dated at ~1020 yr BP. This earthquake is responsible for remobilizing the largest  
16 volume of sediments in the entire stratigraphic sequence of Lake Maskinongé, the  
17 westernmost lake. This earthquake was not recorded in Lake Aux-Sables and St-Joseph,  
18 which are located eastward from Maskinongé, but the largest MMDs are associated with the  
19 well-known 1663 AD event of eastern Québec. Therefore, both earthquake events are  
20 interpreted to have different epicenters and the lakes of southeastern Québec recorded  
21 earthquakes from both seismic zones.

22 Key words: Mass-movement deposits, earthquakes, lakes, geomorphology, stratigraphy

## 23 INTRODUCTION

24 The record of seismic activity prior to colonisation is poorly documented in northeastern  
25 North America, as historic testimonials are limited to the past ~450 years (at best) and data  
26 availability is closely linked to the locations of historical European settlements (Gouin, 2001).  
27 Since the early 20<sup>th</sup> century, geological investigations and instrumental monitoring systems  
28 improved the understanding of seismic activity, providing valuable information on  
29 magnitude, location and recurrence intervals of earthquakes (e.g., Lamontagne, 1987; Adams  
30 and Basham, 1989). However, only limited information is presently available on pre-  
31 colonization seismic events, even though it is critical for determining the recurrence interval  
32 of large infrequent earthquakes (St-Onge et al., 2004; Locat, 2008).

33 Lacustrine basins are depositional environments that can provide detailed information on  
34 significant earthquake events (Sims, 1975; Doig, 1986; Shilts and Clague, 1992; Ouellet,  
35 1997; Chapron et al., 1996, 1999; Schnellmann et al., 2002; Nomade et al., 2005; Strasser et  
36 al., 2006; Arnaud et al., 2007; Chapron et al., 2007; Bertrand et al., 2008; Doughty et al.,  
37 2010a, 2010b; Ledoux et al., 2010; Moernaut and De Batist, 2011; Lauterbach et al., 2012;  
38 Brooks, 2013a, 2013b; Doughty et al., 2014; Brooks., 2016; Locat et al., 2016; Lajeunesse et  
39 al., 2017; Normandeau et al., 2017). The high water content and the poor consolidation of  
40 lacustrine sediments make them sensitive to external disturbance, causing failures (Shilts,  
41 1984; Shilts and Clague, 1992). Many mechanisms can trigger slope disturbances and  
42 subaquatic mass-movements such as water level fluctuations, wave loading, high  
43 sedimentation rates, anthropogenic disturbances and earthquakes (Shilts, 1984; Shilts and  
44 Clague, 1992; De Blasio et al., 2004; Cauchon-Voyer et al., 2008; Fanetti et al., 2008;

45 Duchesne et al., 2010; Normandeau et al., 2013; Smith et al., 2013). Mass-movement  
46 deposits (MMDs) in lakes located near active seismic zones can be a proxy to identify Late-  
47 Pleistocene and Holocene earthquakes (e.g., Brooks, 2016). Many factors can link MMDs to  
48 a seismological trigger, but the key signature is multiple, synchronous-triggered MMDs  
49 (Shilts and Clague, 1992; Schnellmann et al., 2002; Bertrand et al., 2008; Smith et al., 2013;  
50 Brooks, 2015, 2016).

51 MMDs are common in lakes located within and near active seismic zones of eastern Québec  
52 (e.g., Shilts et al. 1992; Ouellet, 1997; Lajeunesse et al., 2008; Doughty et al., 2010a, 2010b,  
53 2013, 2014; Locat et al., 2016; Lajeunesse et al., 2017) where they can be present at multiple  
54 stratigraphic levels. In southern Québec, postglacial MMDs are observed in lakes located  
55 near the CKSZ and are absent in lakes located away from it (Ouellet, 1997), suggesting that  
56 they have been triggered by earthquake events. Ouellet (1997) and Lajeunesse et al. (2017)  
57 proposed that paleoseismological research in eastern Canada should focus on MMDs  
58 occurring outside and away from very active seismic zones to identify high magnitude  
59 seismic events and avoid the background noise induced by frequent smaller earthquakes.

60 High-resolution swath bathymetric imagery allows full-bottom coverage of lacustrine basins  
61 and provides detailed information on lake-bottom morphology and sedimentary processes  
62 such as mass-movements (Locat and Lee, 2002; Hilbe et al., 2011; Strasser et al., 2011;  
63 Normandeau et al., 2013; Smith et al., 2013; Hilbe and Anselmetti, 2014). Older deglacial  
64 and postglacial MMDs in the stratigraphy can be identified on sub-bottom profiles. An  
65 approach combining high-resolution swath bathymetric imagery and sub-bottom profiles can  
66 provide valuable information on the spatial distribution of MMDs over an entire lake basin

67 (e.g., Praet et al., 2016; Lajeunesse et al., 2017). In addition, sediment core data allow dating  
68 possibilities through depositional rates and can thus lead to a better understanding of  
69 paleoearthquakes.

70 This paper presents a morpho-stratigraphic analysis of three lakes located north of the St.  
71 Lawrence River, southern Québec (Canada), within the limits of the former deglacial  
72 Champlain Sea. The lakes are located between the WQSZ and the CKSZ (Fig. 1b) and  
73 provide insights into the deglacial and postglacial history of paleoseismic activity for the area  
74 between the major urban centres of Québec City and Montréal. More specifically, it aims to  
75 1) describe the geomorphology and distribution of MMDs in these lacustrine basins; 2)  
76 identify the triggering factors of mass-movements; and 3) provide a chronostratigraphic  
77 framework for mass-movements in these lakes.

## 78 **STUDY AREA**

### 79 *Physical setting*

80 Lakes Maskinongé, Aux-Sables and St-Joseph, southern Québec (Table 1), are located  
81 within the Grenville geological province of the Canadian Shield, where bedrock mainly  
82 consists of Precambrian metamorphic and igneous rock (Geological Survey of Canada,  
83 2008). During the last glaciation, the lake basins were all covered by the Laurentide Ice-  
84 Sheet (LIS) and were entirely deglaciated by ~13 ka cal. (Occhietti et al., 2011). The small  
85 and shallow basins are all located below marine limit ( $\leq 210$  m asl in the region) (Parent and  
86 Occhietti, 1988; Normandeau et al., 2013, 2017) (Fig. 1b) and were emerged from the sea  
87 by ~10 ka cal BP (Parent and Occhietti, 1988). The lakes were selected for this study because

88 previous investigations highlighted the widespread occurrence of MMDs on their floors  
89 (Ouellet, 1997; Normandeau et al., 2013, 2017).

90 **Table 1**

91 Physical characteristics of the investigated lakes.

92

93 Lake Maskinongé is a circle-shaped basin and its main tributary is the Mastigouche River  
94 located at the northern end of the lake. Lake Aux-Sables is 5.2 km long, has a maximum  
95 width of 1 km and is oriented from NE to SW. Its sedimentary input comes from multiple  
96 small streams, but there is no major tributary. Lake St-Joseph has a length of 7 km and a  
97 maximum width of 3 km. The lake is composed of two main basins. Its main tributary is the  
98 Rivière-aux-Pins that discharges into the northern basin of the lake. The three lakes  
99 stratigraphic successions were previously investigated and seven Late-Pleistocene and  
100 Holocene units were identified ranging from deglacial marine to postglacial lacustrine  
101 sediments (Normandeau et al., 2013, 2017).

102 *Regional seismicity*

103 Eastern Canada is part of a mostly aseismic stable craton with some restricted zones showing  
104 seismological activity (Fig. 1a). Three of these zones are partly located in the province of  
105 Québec and are all related to the reactivation of the Iapetan rift fault system, known as the  
106 St. Lawrence rift system (Adams and Basham, 1989; Tremblay et al., 2013). These three  
107 zones are: i) the Western Québec seismic zone (WQSZ), where earthquake epicentres are  
108 mostly distributed in eastern Ontario, western Québec and northern New-York state; ii) the  
109 Charlevoix-Kamouraska seismic zone (CKSZ), centered in the St. Lawrence Estuary, south

110 of the Saguenay fjord (Fig. 1), and iii) the Lower St. Lawrence seismic zone (LSLSZ), located  
111 in the eastern part of the St. Lawrence Estuary, which has a low activity of small magnitude  
112 earthquakes (Adams and Basham, 1989; Locat, 2011). The WQSZ and the CKSZ are also  
113 partly due to local crustal fractures resulting from a passage over a hot spot during the  
114 Cretaceous and a meteoritic impact structure, respectively (Adams and Basham, 1989). The  
115 WQSZ is divided in two areas: a SE-NW band extending from Montréal to the upper  
116 Gatineau River and a less active southern band with epicenters located along the Ottawa  
117 River (Adams & Basham, 1989). Many historical earthquakes have been documented in the  
118 WQSZ, with events reaching  $M=5$  to  $M=6$  (Fig. 1: 1732 AD,  $M5.8$ ; 1935 AD,  $M6.2$ ; 1944  
119 AD,  $M5.8$ ) (Natural Resources Canada, 2018). The CKSZ, southeastern Québec, is the most  
120 active seismic zone in eastern Canada (Fig. 1a), with many historical earthquakes reaching  
121  $M \geq 6$  (Fig. 1: 1663 AD,  $M>7$ ; 1860 AD,  $M6$ ; 1870 AD,  $M6.5$ ; 1925 AD,  $M6.2$ ; 1971 AD,  
122  $M6$ ) (Lamontagne, 1987; Adams and Basham, 1989; Doig, 1998; Tuttle and Atkinson, 2010;  
123 Locat, 2011).

124 The region in which the three studied lakes are located is bounded by the two most important  
125 seismic zones of eastern Canada (WQSZ and CKSZ) (Fig. 1a, b), exposing it to a recurrence  
126 of seismic events since deglaciation. Although only few historical earthquakes occurred in  
127 the WQSZ, analysis of the disturbance of lacustrine sediment has linked deposits in the  
128 Outaouais region to the 1935 AD seismic event (Shilts, 1984; Shilts and Clague, 1992;  
129 Doughty et al., 2010a, 2010b). Cores analysis from lacustrine basins also allow Doig (1986,  
130 1991, 1998) to identify past earthquakes. Additionally, pre-historical seismic events (7060  
131 yr BP, 4550 yr BP and 1020 yr BP) from the WQSZ were identified by analysing and dating

132 large terrestrial landslides (Aylsworth et al., 2000; Brooks, 2013a, 2013b). By contrast, the  
133 CKSZ has an approximate recurrence rate of 70 years for earthquakes of magnitude  $M \geq 6$   
134 (Ouellet, 1997; Natural Resources Canada, 2018). Ouellet (1997) observed that the largest  
135 sublacustrine disturbances occurred usually within a radius of  $34.5 \pm 5$  km from the CKSZ.  
136 Physical damage to infrastructures has also been reported in the literature at a distance of 180  
137 km to over 800 km from the epicenter of an earthquake of magnitude  $\geq 7$  (Ouellet, 1997;  
138 Geological Survey of Canada, 2001). Deglacial and postglacial seismic events were also  
139 identified by Tuttle and Atkinson (2010) dated at 10.12-9.41 ka yr BP and 5.04 ka yr BP in  
140 the Charlevoix region, and an event around 7.25 ka yr BP was dated by Cauchon-Voyer  
141 (2008) in the St. Lawrence Estuary.

## 142 **MATERIAL AND METHODS**

### 143 *Hydroacoustic survey*

144 Hydroacoustic surveys were undertaken in the three lakes between 2011 and 2014 to acquire  
145 high-resolution swath bathymetry imagery and sub-bottom profiles. The hydroacoustic  
146 database presented in this paper is the same as the one used by Normandeau et al. (2013,  
147 2017). Data was acquired using two different swath bathymetric systems, depending on lake  
148 depth and accessibility. In the shallow southern basin of Lake St-Joseph ( $< 20$  m), data was  
149 acquired with an *Odom ES3* multibeam echosounder (240 kHz), together with an *Ixsea*  
150 *Octans III* motion sensor and an *SX Blue* DGPS ( $\sim 60$  cm precision). The other lakes were  
151 mapped with a *GeoAcoustics GeoSwath Plus Compact* interferometric bathymetric sonar  
152 (250 kHz), coupled with a *Valeport SMC* motion sensor and a *Hemisphere V101* DGPS ( $\sim$   
153 60 cm precision) for positioning. The instruments were mounted on two different platforms;

154 an inflated boat (Zodiac) and a pontoon boat. Bathymetric data were post-processed using  
155 *Caris Hips and Sips 8.1* software.

156 Acoustic stratigraphy data was acquired using a dual frequency *Knudsen 3212* (3.5 and 12  
157 kHz) sub-bottom profiler; refer to Figures 3A, C, D of Normandeau et al. (2017) for the  
158 profiling survey pattern. Survey lines were planned perpendicularly to each other in order to  
159 better visualize the distribution of the acoustic units in the lake basins. A sound velocity of  
160  $1500 \text{ m s}^{-1}$  was used to compute depths and sediment thickness. The *SegyJp2Viewer* software  
161 from Natural Resources Canada (NRCan) and *SonarWiz 5.0* were used to analyze the sub-  
162 bottom profiles which were then coupled to the high-resolution bathymetric imagery using  
163 the *QPS Fledermaus* software.

#### 164 *Sedimentological analysis*

165 Short cores (< 1.5 m; Table 2) were collected with a percussion corer from an ice surface  
166 during winter at all of the studied lakes. Based on the sub-bottom profile dataset, one coring  
167 site in each lake was chosen to sample recent undisturbed sediments to get a deposition rate  
168 through  $^{210}\text{Pb}$  radiometric activity. Cores were analyzed through a CT-Scan at the Institut  
169 National de la Recherche Scientifique Centre Eau Terre Environnement (INRS-ETE) in  
170 Québec City and then split, visually described and photographed. Magnetic susceptibility  
171 (MS) was measured manually every centimeter using a *Bartington MS3*.

172 Samples were collected in cores at every centimeter on the upper 15 cm for  $^{137}\text{Cs}$  and  $^{210}\text{Pb}$   
173 radiometric analyses. The sedimentation rates (SR), assuming a constant rate, were calculated  
174 using:

$$175 \quad \text{SR} = - [(\ln(2))/(\text{Slope} * 22.3)]$$

176 (e.g., Gagné et al., 2009; Duboc et al., 2016). No samples from a depth deeper than where  
177 the non-supported  $^{210}\text{Pb}$  activity values reach the supported  $^{210}\text{Pb}$  activity values were used  
178 to calculate each respective sedimentation rates. On the other hand, the radiometric activity  
179 of  $^{137}\text{Cs}$  allowing sediment deposited in 1963 AD to be identified by the peak activity of  $^{137}\text{Cs}$   
180 attributed to the atmospheric nuclear bomb testing (Arnaud et al., 2002). Radiometric activity  
181 was measured on every samples at the Laboratoire de Radiochronologie of the Centre  
182 d'études nordiques (U. Laval).

### 183 **Table 2**

184 Description and location of cores collected in the investigated lakes.

185

## 186 **RESULTS**

### 187 *Lake bottom morphology*

188 High-resolution swath bathymetric imagery reveals similar morphologies on the lake basin  
189 floors at all three lakes: headwall scarps, gullies, lobe of hummocky debris and hummocky  
190 topographies (Fig. 2). These morphologies are typical of lacustrine basins affected by mass-  
191 movements (e.g., Hampton and Locat, 1996; Moernaut and De Batist, 2011). These  
192 observations are also coherent with results of previous studies that highlighted that the  
193 studied lakes are affected by mass-movements (Ouellet, 1996; Normandeau et al., 2013,  
194 2017). Therefore, the above morphological criteria (Fig. 2) are here used to identify MMDs  
195 on the high-resolution swath bathymetric imagery.

196 *Acoustic stratigraphy*

197 For the purpose of this study, the seven acoustic units previously identified in the three lakes  
198 by Normandeau et al. (2013, 2017) have been grouped into three main depositional units,  
199 providing a stratigraphic framework (Fig. 3). Ua located at the bottom of the stratigraphic  
200 sequence lacks acoustic penetration and is interpreted as ice-contact sediments (till) or  
201 bedrock. Ub is a thick acoustically transparent unit overlaid by high amplitude parallel  
202 reflections and groups U3 and U4 of Normandeau et al. (2013). This unit results from the  
203 high sedimentation rates of the glaciomarine environment of the Champlain Sea during rapid  
204 ice margin retreat (Normandeau et al., 2013). Uc has low amplitude parallel reflections and  
205 is associated with paraglacial and postglacial sedimentation; it groups U5, U6 and U7 of  
206 Normandeau et al. (2013, 2017).

207 These three units are observed in Lake Aux-Sables and Lake St-Joseph, but the acoustic  
208 attenuation in the sediments limited the signal penetration down to Ua in Lake Maskinongé.  
209 However, Ub and Uc are identified in every investigated lake. MMD acoustic facies is  
210 observed in Ub and Uc: it is acoustically transparent to chaotic, has a hummocky topography,  
211 an erosive base and a lense geometry (Fig. 3).

212 *Lake Maskinongé*

213 The high-resolution bathymetric map of Lake Maskinongé (Fig. 4a) reveals three distinct  
214 types of lake floor morphologies (Fig. 4b): 1) a flat smooth surface; 2) linear to sinuous  
215 structures from 50 to 100 m wide and ~600 m long, appearing slightly shallower ( $\leq 1$  m) and  
216 in topographic unconformity with the flat bottom floor; and 3) widespread mass-movement  
217 surface morphologies, such as hummocky topography, displaced blocks, scarps on the

218 southeastern margins and lobes of hummocky debris extending away from the lateral slopes.  
219 The linear to sinuous structures all converge towards the deep basin and are located on the  
220 northern slope at the front of the Mastigouche River mouth. MMDs are all coalescent,  
221 forming one large-scale chaotic area on the lake bottom, covering the base of the western,  
222 southern and eastern slopes of the lake (Fig. 4b). MMD morphologies cover 4.09 km<sup>2</sup>, which  
223 represents 40% of the lake basin surface.

224 The sub-bottom profiles show the acoustic facies of the deposits underlying the topographic  
225 morphologies (Fig. 5). Below the smooth flat bottom floor lies 4 m of continuous parallel  
226 reflections (Uc). Sub-bottom profiles show a lateral unconformity under the morphological  
227 linear to sinuous structures where the parallel reflections are acoustically chaotic and  
228 vertically offset. Lenses of acoustically chaotic sediments associated with MMD facies are  
229 visible at three different intervals within the acoustic sequence. These lenses are observed at  
230 depth of 5.5-6.0 m (Event ME1 within Ub), 1.5 m (Event ME2 within Uc) and 0.5-1.0 m  
231 (Event ME3 within Uc), indicating three distinct mass-movement events. The acoustic  
232 attenuation in the sediment made it impossible to delineate the base of the first and second  
233 deposit of mass-movement on all of the sub-bottom profiles. In this case, MMDs overly  
234 directly the acoustically transparent glaciomarine unit (Ub). However, ME2 deposit underlies  
235 the extensive hummocky topography observed on the swath bathymetric imagery (Fig 6), as  
236 ME3 is associated with small MMD lenses located only at the base of slopes. Based on the  
237 sub-bottom profiles where the bottom of ME2 is observed, the deposits ME2 and ME3 reach  
238 a maximal thickness of 7 m and 1.5 m, respectively. The isolated displaced blocks are  
239 characterized on sub-bottom profiles by high-amplitude parallel reflections and sharp vertical

240 sidewalls. The displaced blocks rise up 4.5 m above the MMDs (Fig. 5b) and the parallel  
241 reflections indicate that they are areas of remnant sediments not displaced by mass-  
242 movements.

243 At a location selected from the analysis of the sub-bottom profiles, a short core (MAS15-  
244 1aP), 105 cm long, was collected at a strategic undisturbed location in Uc (Fig. 7). Structures  
245 caused by the freezing of the sediment during core collection appear as black areas on the  
246 CT-Scan images.  $^{210}\text{Pb}$  profile of Lake Maskinongé is non-linear and the values between the  
247 depth of 6.25 cm and 8.25 cm are probably related to a rapid sedimentation event and were  
248 excluded from the calculation of the depositional rate (Fig. 8). The peak activity of  $^{137}\text{Cs}$   
249 measured in the core is observed at a depth of 7.25 cm, while the  $^{210}\text{Pb}$  radiometric activity  
250 reveals a depositional rate of  $0.18 \text{ cm yr}^{-1}$  (Fig. 8). The depositional rate obtained by the  $^{210}\text{Pb}$   
251 radiometric dating methods is in good agreement with  $^{137}\text{Cs}$  peak activity. A layer (ML1)  
252 with high CT-numbers values is observed in the upper part at a depth of 8.5 cm (~ 12 cm  
253 thick) and also corresponds to high MS values (Table 3, Fig. 7). Such high values indicate a  
254 detrital source of sediment rather than organogenic material. According to the calculated  
255 depositional rate, the layer ML1 is dated at ~1969 AD.

256 **Table 3**

257 Depth, thickness and date of the layers observed in each core.

258

259 *Lake Aux-Sables*

260 Analysis of the high-resolution swath bathymetric imagery of Lake Aux-Sables (Fig. 9a)  
261 reveals two main types of lake bottom morphologies (Fig. 9b): 1) a smooth lake bed surface,

262 present on the flat basin floor and on the slopes; and 2) the widespread occurrence of MMD  
263 surface features in the basin. The smooth lake bed surface is observed in southeastern and  
264 northern sectors of the lake. MMD features are mostly concentrated in the south-central  
265 sector of the lake, but a few small isolated morphologies are also observed in its northern  
266 sector. MMD structures are located at the base of the slopes and are characterized by a  
267 hummocky topography. Headscarps and gullies are typical morphologies observed on the  
268 lake slopes (Fig. 10). Lobes of hummocky debris are also splayed from the lateral sidewalls  
269 onto the central basin. MMD surface morphologies cover 1.8 km<sup>2</sup>, representing 35% of the  
270 lake surface.

271 Sub-bottom profiles (Fig. 11) show an uppermost unit (Uc) acoustically transparent on the  
272 lake lateral shelves, as MMDs facies are observed in the deep basin (Event SE1 within Uc).  
273 Uc has a smooth topography and drapes the underlying glaciomarine unit (UB) conformably,  
274 while MMDs facies has a hummocky topography and a sharp erosive contact at its base.  
275 MMDs of the event SE1 reach a maximum thickness of 5 m on the sub-bottom profiles. No  
276 sediment apparent on the sub-bottom profile are observed over the MMDs of event SE1,  
277 suggesting that the MMDs are modern in age or have the same acoustic signature as the  
278 overlying gyttja deposit.

279 A sediment core (LAS15-1P), 131 cm long, was collected in Lake Aux-Sables in the  
280 undisturbed Uc (Fig. 7). <sup>210</sup>Pb profile of Lake Aux-Sables is non-linear due to biological  
281 mixing at the surface (Fig. 8). Thus, the two surficial values were excluded from the  
282 calculation of the sedimentation rate. The <sup>210</sup>Pb radiometric activity reveals a depositional  
283 rate of 0.08 cm yr<sup>-1</sup>, which is in general agreement with the peak activity of <sup>137</sup>Cs observed

284 at a depth of 5.75 cm (Fig. 8). Layers of high CT-numbers values are observed at a depth of  
285 5.5 cm (SL1), 23 cm (SL2) and 35 cm (SL3) in LAS15-1P, with a respective thickness of 4.5  
286 cm, 5.5 cm and 6 cm (Table 3, Fig. 7). Such depths suggest a deposition of the detrital layers  
287 around 1947 AD (SL1), 1785 AD (SL2) and 1704 AD (SL3); note that the thickness of the  
288 layers was subtracted from the depth to calculate the ages. The MS in core LAS15-1P is  
289 highly variable and only the second layer of high CT-number values (SL2, 23 cm)  
290 corresponds to a small increase of MS.

### 291 *Lake St-Joseph*

292 The northern and southern basins of Lake St-Joseph are isolated from each other by a 2-m  
293 deep central sill (Fig. 12a, b); both have distinct morphologies and bathymetries. The  
294 southern basin has a flat and uniform shallow lake bottom morphology ( $\leq 12$  m); the northern  
295 basin is deeper ( $\leq 37$  m) with widespread MMD surface morphologies. Mass-movement  
296 morphologies observed on the bathymetry imagery include headscarps, residual mounds,  
297 hummocky topography and compression ridges caused by frontal thrusting (Fig. 12b, 13).  
298 The hummocky areas of MMDs in the northern basin originated from the northeastern,  
299 southern and eastern slopes and coalesce on the basin-floor. They cover 2.8 km<sup>2</sup>, representing  
300 36% of the basin surface.

301 Three different stratigraphic levels of MMDs are observed on the sub-bottom profiles in Ub  
302 and Uc, indicating distinct mass-movement events (Fig. 14). Two stacked transparent to  
303 chaotic lenses (MMD Facies) are observed in a topographic depression at the base of the  
304 western slope, buried under 5.5 m of sediments (Events JE1 & JE2 within Ub). A third  
305 acoustically transparent to chaotic lens associated with MMD facies is located at the base of

306 the eastern slope (Event JE3 within UC). This thick ( $\leq 10$  m) lens underlies hummocky  
307 topography and has a sharp erosive base. The interface between the uppermost MMDs (JE3)  
308 and Ub is characterized by a high-amplitude acoustic reflection. Compression ridges  
309 associated with frontal thrusting are located at the distal part of MMDs. These ridges make a  
310 lateral transition between MMDs facies and the undisturbed acoustically laminated Uc. The  
311 thick JE3 MMD is covered by 0.5-1.0 m of sediment (Fig. 14a, c).

312 Core LJS15-1bP, 123 cm long, was collected in the northern basin in an undisturbed sector  
313 of Uc (Fig. 7). The  $^{210}\text{Pb}$  activity indicates a depositional rate of  $0.07 \text{ cm yr}^{-1}$ , which is in  
314 good agreement with the  $^{137}\text{Cs}$  activity at a depth of 3.25 cm (Fig. 8). Layers of high CT-  
315 number and MS values are observed at a depth of 19 cm (JL1) and 49 cm (JL2), with a  
316 respective thickness of 3.5 cm and 1 cm (Table 3, Fig. 7). According to the depositional rate,  
317 these layers are dated at  $\sim 1745$  AD (JL1) and  $\sim 1366$  AD (JL2).

## 318 **DISCUSSION**

### 319 *Seismicity as a trigger of mass-movements*

320 Sediments of the three lakes show evidence of mass-movements that, in terms of area and  
321 volume, mostly affected the late-deglacial and postglacial units (Uc: ME2, ME3, SE1 & JE3),  
322 although buried MMDs were observed in the glaciomarine unit (Ub: ME1, JE1 & JE2)  
323 deposited during deglaciation. Even though the basins are all located within the area of two  
324 active seismic zones and are all widely affected by mass-movements, it is necessary to  
325 consider every possible trigger mechanism before concluding to a seismic trigger.

326 High water level variations can trigger slope failures. In the studied area, such variations

327 were limited to the deglacial Champlain Sea transgression and forced regression (from 11.1  
328 cal. Ka BP to 10.5 cal. ka BP) (Occhietti and Richard, 2003), and no major water level  
329 fluctuation occurred since the establishment of the postglacial drainage network.  
330 Additionally, in contrast to open sea water, lacustrine environments are not subject to high  
331 wave energy on shoreline. The studied lakes also have a relatively small surface area (from  
332 5.2 km<sup>2</sup> to 11.3 km<sup>2</sup>) reducing the fetch and the possibility to generate strong erosive waves.  
333 Therefore, the modern-aged MMDs observed in Uc were most probably not triggered by  
334 major water level variations or wave loading on the shoreline. Conversely, it is not excluded  
335 that the MMDs observed within the glaciomarine unit (Ub) could have been triggered by a  
336 major water level variation although wave loading would be unlikely since the basins were  
337 situated in isolated bays during the regression.

338 The MMDs surface morphologies observed on the swath bathymetric imagery indicate that  
339 the disturbed slopes of Lake Maskinongé are not connected to sectors receiving a higher  
340 sedimentary input. In fact, the disturbed slopes are located on the opposite side of the lake,  
341 whereas the slopes located at the river mouth are the only ones that do not show scarps or  
342 MMDs. Lake Aux-Sables disturbed slopes are also not associated with a high sedimentation  
343 rate, having no main river input but many small streams instead. The northern basin of Lake  
344 St-Joseph is also widely affected by mass-movements but, even though scars are observed  
345 on the swath bathymetric imagery near the river discharge, the disturbed area extends far  
346 from the delta. However, the surface features observed on the swath bathymetric imagery are  
347 only relevant to the modern-aged events. In the studied lakes, late postglacial slope failures  
348 deposited within Uc are not associated with an overload resulting from high depositional

349 rates near a river discharge because 1) the majority of the disturbed slopes observed on the  
350 swath bathymetric imagery are located far from deltas and 2) the lakes are all characterized  
351 by modern low depositional rates (from  $0.07 \text{ cm yr}^{-1}$  to  $0.18 \text{ cm yr}^{-1}$ ). However, overloading  
352 is not excluded as a trigger for the buried MMDs observed within the glaciomarine unit (Ub:  
353 ME1, JE1 & JE2), since 1) deglacial times were characterized by higher sedimentation rates  
354 (Normandeau et al., 2013, 2016) and 2) the setting of each lake was different at that time,  
355 being deeper basins during the Champlain Sea transgression and having different location of  
356 sedimentary input.

357 From the analysis of the swath bathymetric imagery, MMDs are widespread in the lake basins:  
358 they extend over a total of 34% to 40% of the surface of the three lakes. According to the  
359 high-resolution swath bathymetric imagery and the acoustic sub-bottom profiles analysis,  
360 synchronous events occurred within each lake respectively: headwall scarps are observed on  
361 different slope orientations and many MMDs are observed within the same stratigraphic unit.  
362 The MMDs of events ME2, SE1 and JE3 corresponding to widespread disturbed topography  
363 on the lake floors indicate that synchronous events triggered the slopes failures of more than  
364 one sidewall and formed one large-scale coalescent MMD or many isolated smaller MMDs  
365 in each respective lake. The MMDs of event ME3 do not cover a wide surface area, but are  
366 observed at the base of many slopes indicating that small synchronous failures occurred.

367 Based on the synchronicity of multiple mass-movements (e.g. Schnellmann et al., 2002;  
368 Fanetti et al., 2008; Doughty et al., 2010b) and considering that the lakes are all located  
369 within the area of two active seismic zones, mass-movements events ME2, ME3, SE1 and  
370 JE3 are interpreted to be seismically induced. Similarly, *in situ* disrupted horizontal parallel

371 reflections within a particular layer have been attributed to liquefaction induced by a nearby  
372 strong seismic shaking (Shilts et al., 1992; Beck, 2009; Tuttle and Atkinson, 2010). The linear  
373 to sinuous structures observed on the swath bathymetric imagery and on acoustic subbottom  
374 profiles at the Mastigouche River mouth in Lake Maskinongé are interpreted as liquefaction  
375 features since sub-bottom profiles show lateral unconformity in the acoustic draping parallel  
376 reflections indicating that the sediments were fluidilized in situ (Shilt et al., 1992). These  
377 disrupted reflections in upper Uc suggest that a strong modern-aged earthquake might have  
378 disturbed the sedimentary infill in Lake Maskinongé. However, other possible aseismic  
379 triggers are still considered for the deglacial mass-movement events ME1, JE1 and JE2 since  
380 depositional environments were highly different at that time.

#### 381 *Deglacial and postglacial seismicity*

382 The stratigraphy and distribution of MMDs in the investigated lakes are here used to  
383 reconstruct the history of major seismic events since deglaciation. The  $^{210}\text{Pb}$  depositional  
384 rates provided a chronological framework, but the proposed chronology represents a minimal  
385 age of the events because: 1) only the upper 15 cm of sediments were used to calculate the  
386 mean depositional rates and then applied to a depth ranges of 0.5-1.5 m; 2) compaction in the  
387 sediments occur with time, implying that the  $^{210}\text{Pb}$  radiometric dating overestimates the  
388 depositional rates; 3) a mean sound velocity of 1500 m/s was used to calculate the time-  
389 travelling depths and no sound velocity correction was applied for the sedimentary column;  
390 and 4) measures of depths on the sub-bottom profiles have a precision of  $\sim 0.5$  m.

391 MMDs in the lakes occur along three distinct stratigraphic levels, indicating three different  
392 phases of mass-movements (Fig. 5 & 14, Table 4): deposits of Phase 1 (ME1, JE1 & JE2)

393 are in the glaciomarine unit (Ub), and deposits of phases 2 (ME2) and 3 (ME3 & JE3) are in  
394 the upper part of the paraglacial and postglacial unit (Uc) and are separated by 0.5-1.0 m of  
395 undisturbed sediments. The stratigraphic position of the MMDs of Phase 1 observed in Ub  
396 in Lake Maskinongé and St-Joseph indicates a triggering mechanism during the deglacial  
397 Champlain Sea probably related to the rapid initial glacio-isostatic rebound (Normandeau et  
398 al., 2013; Lajeunesse, 2016). Normandeau et al (2017) also highlighted 9 stacked MMDs  
399 buried in Ub in Lake Aux-Sables. Brooks (2016) suggested that seismic activity can be  
400 increased during deglaciation due to the crustal deformation during glacio-isostatic rebound.  
401 The buried MMDs are probably associated with the same series of diachronic events that  
402 took place during the retreat of the LIS margin, according to each lake basin respective timing  
403 of deglaciation. A phase of enhance mass-movement events thus likely occurred around 11.1  
404 to 10.5 cal. Ka BP, during the deglacial Champlain Sea episode, most probably triggered by  
405 local seismic activity caused by the rapid initial glacio-isostatic rebound. However, deglacial  
406 times were characterised by depositional environments of higher energy, sedimentation rates  
407 and water level variation (Normandeau et al., 2013, 2017), which could also precondition the  
408 sediments to slope failures (Lajeunesse and Allard, 2002).

409 The MMD associated to Phase 2 (ME2) is only observed in Lake Maskinongé (Table 4), at  
410 a depth of 1.5 m in the postglacial unit (Uc). The extrapolated  $^{210}\text{Pb}$  depositional rate over  
411 the sedimentary column in the Lake Maskinongé indicates that an earthquake occurred  
412 around or before 1180 AD. Brooks (2013a) also dated a large-scale terrestrial landslide ( $\sim 31$   
413  $\text{km}^2$ ) in Quyon Valley, near the WQSZ, at  $\sim 1020$  yr BP and a minimal magnitude of  $M \sim 6.1$   
414 was estimated. Based on the dating proximity and the intensity of the seismic shock, we

415 suggest that the MMD associated to Phase 2 (ME2) relates to the same event recorded in  
416 Quyon Valley, indicating that a strong earthquake ( $M \geq 6.1$ ) from the WQSZ disturbed Lake  
417 Maskinongé sedimentary sequence around  $\sim 1020$  yr BP. However, Lake Aux-Sables and  
418 Lake St-Joseph stratigraphic sequences did not record that event most probably because they  
419 are located farther away from the WQSZ (235 km and 290 km, respectively).

420 Similarly, the deposit of the third and last phase of mass-movement (ME3 & JE3) is observed  
421 in the same paraglacial and postglacial unit (Uc) at a depth of 0.5-1.0 m in Lake Maskinongé  
422 and St-Joseph (Table 4). This MMD was cored by Normandeau et al (2013) at a depth of  
423 0.23 cm in Lake Saint-Joseph and dated with bulk sediment at 1250 AD. However, we revise  
424 this date since the correlation between bulk sediment dating and a given MMD can be low  
425 and such a depth indicate a timing event around 1685 AD using our new depositional rate of  
426  $0.07 \text{ cm yr}^{-1}$ . According to the depth of the MMDs ME3 & JE3, it seems unlikely that those  
427 events relate to the strong ( $M 6.2$ ) historical earthquake that occurred in 1935 AD in the  
428 WQSZ (Doughty et al., 2010b). We rather suggest that the deposits of ME3 & JE3 are  
429 associated with the  $M > 7$  1663 AD CKSZ earthquake, since it was the strongest historical  
430 event ever recorded in eastern Canada (Locat, 2002). The MMDs of event SE1 in Lake Aux-  
431 Sables are most probably related to the same earthquake (CKSZ  $M > 7$ , 1663 AD) since 1)  
432 the lake is located between Lake Maskinongé and St-Joseph, which basins recorded the  
433 seismic shock, and 2) the highly chaotic topography of Lake Aux-Sables indicates a modern-  
434 aged event. However, it is not clear if the MMDs either are recent or have the same acoustic  
435 signature as the overlying gyttja deposit because no sediment apparent on the sub-bottom  
436 profile returns are observed over the MMDs.

437 **Table 4**

438 Summarize of the three phases of mass-movements with their respective deposits, date and seismic  
439 trigger event.

440

441 The seismic events reported by Tuttle and Atkinson (2010) dated at 5.04 ka yr BP in the  
442 Charlevoix region and the one reported by Cauchon-Voyer (2008) at 7.25 ka yr BP in the St.  
443 Lawrence Estuary are not observed in the sedimentary record of the three studied lakes,  
444 suggesting epicenters located farther to the east. The pre-historic WQSZ events reported by  
445 Aylsworth et al. (2000) dated at 7060 yr BP and 4550 yr BP were not recorded in the  
446 stratigraphy of the studied lakes, neither is the strong recent historical earthquakes of the  
447 WQSZ (1935 AD, M 6.2).

448 *Scale of the deposits*

449 The deposits related to Phase 2 in Lake Maskinongé (ME2) represent the main mass-  
450 movement structures in its entire acoustic stratigraphy. The deposits of phase 2 (ME2) is  
451 thicker than the deposits of Phase 3 (ME3) (7 m v.s 1.5 m thick, respectively), even if the  
452 earthquake of Phase 2 is believe to be of smaller magnitude than the event of Phase 3 ( $M \geq$   
453 6.1 vs  $M \geq 7$ , respectively). Conversely, the CKSZ  $M > 7$  1663 AD event triggered the biggest  
454 MMD structures in Lake Aux-Sables (SE1,  $\leq 5$  m thick) and in Lake St-Joseph (JE3,  $\leq 10$  m  
455 thick). It was previously mentioned that Lake Aux-Sables and St-Joseph were not submitted  
456 to seismic disturbances during the event of phase 2 of the WQSZ because the lakes are located  
457 too far away. The difference of thickness between the deposits of each seismic events indicate  
458 that the recurrence rate of strong earthquakes controls the ability of a lacustrine basin to  
459 record seismic shaking by reducing the sediment availability to form wide mass-movement

460 deposits under strong seismic shaking (Wilhelm et al., 2016), in favor of frequent smaller  
461 deposits instead. In Lake Maskinongé, MMDs of the event ME3 are much smaller than the  
462 MMDs of the event ME2 because the failure that occurred some 600 years earlier reduced  
463 the sediment availability to generate a large-scale MMDs. Therefore, MMDs associated with  
464 a seismic event are not necessarily representative of the intensity or the proximity of an  
465 earthquake because the recurrence interval affects sediment availability. In order to identify  
466 the intensity of past earthquakes, investigations need to contextualize the seismically induced  
467 MMDs in a regional stratigraphic framework and to consider the recurrence rates of strong  
468 earthquakes.

#### 469 *RAPIDLY DEPOSITED LAYERS*

470 In contrast with the normal organogenic lacustrine sedimentation, high MS values associated  
471 with high CT-numbers values in cores indicate a detrital source of material. These layers are  
472 referred here as rapidly deposited layers (RDLs). Similar thin silt layers were observed by  
473 Doig (1986) in lakes located in southern Québec and were interpreted to result from the fine  
474 grained particles kept in suspension by water oscillation during a sublacustrine mass-  
475 movement. Doig (1986) interpreted the RDL as seismically induced due to the proximity of  
476 an active seismic zone and to the absence of organic material near the layers, excluding the  
477 possibility of flooding. RDLs are also reported in the Saguenay Fjord and were interpreted  
478 as turbidites (St-Onge et al., 2004; St-Onge et al., 2012).

479 In Lake Maskinongé, the RDL ML1 observed at a depth of 8.5 cm (1969 AD) in core  
480 MAS15-1aP could result from a terrestrial 1950 AD mass-movement (ArchivesCanada) that  
481 occurred in the glaciomarine silty-clay along the shore of the Mastigouche River, the main

482 tributary of the lake. RDLs observed in lacustrine basins are thus not systematically  
483 associated with an earthquake, even if the lakes are located near active seismic zones as the  
484 entire watershed dynamics need to be considered in order to identify the trigger of such layers  
485 in a lake basin. Conversely, the RDL SL1 dated at ~1947 AD in Lake Aux-Sables could be  
486 of seismic origin because two significant earthquakes occurred in the WQSZ during the first  
487 half of the 20<sup>th</sup> century (1935 AD, M 6.1; 1944 AD, M 5.8) (Natural Resources Canada,  
488 2018). Similarly, the RDL JL1 in Lake St-Joseph dated at ~1745 AD could have been trigger  
489 by the WQSZ 1732 AD (M 5.8) event. No historical earthquakes seem to relate to the RDLs  
490 SL2 and SL3 in Lake Aux-Sables and JL2 in Lake St-Joseph, dated at ~1785 AD, ~1704 AD  
491 and ~1366 AD, respectively. However, even if a seismic trigger is possible for the RDLs  
492 SL1, SL2 and JL1, other local or inter-basin trigger mechanisms such as flood or  
493 anthropogenic disturbances are also possible. The RDLs do not show the synchronously-aged  
494 multiple deposits key signature of a seismic trigger and our investigations were aimed on  
495 only one core from each lake. RDLs might not be recorded in the entire lake basin area,  
496 suggesting that single coring investigations do not necessarily provide information on the  
497 disturbance rate of a lacustrine basin and paleoseismological investigations should focus on  
498 multiple cores sampled from different sites. Coring investigations aiming to reconstruct the  
499 history of seismically induced RDLs should also take place away from the sedimentary input  
500 of the river mouth.

## 501 **CONCLUSIONS**

502 High resolution swath bathymetric imagery, sub-bottom profiler and sediment core data  
503 collected in three lakes (Maskinongé, Aux-Sables and St-Joseph) located near two active

504 seismic zones (WQSZ and CKSZ) in south-central Québec reveal that the lacustrine basins  
505 were highly disturbed by three distinct phases of seismically-induced mass-movements since  
506 deglaciation, without any event between late-deglacial and late postglacial times. These  
507 mass-movements are interpreted to have a seismic triggering due to 1) the widespread  
508 distribution of MMDs, covering  $\geq 34\%$  of each lacustrine basin area; 2) the presence of  
509 disturbed slopes with headwall scarps located far from a sedimentary input; 3) the occurrence  
510 of many MMDs along the same stratigraphic level, suggesting synchronous events; and 4)  
511 the presence of liquefaction structures observed on sub-bottom profiles.

512 MMDs were observed at different stratigraphic levels on sub-bottom profiles of the  
513 investigated lakes, allowing the identification of three different phases of seismic events.  
514 Taken together, the stratigraphic position of the MMDs and the depositional rates suggest  
515 that: Phase 1 occurred during the deglacial Champlain Sea episode (11.1 to 10.5 cal. Ka BP)  
516 and produced many mass-movements, when rates of glacio-isostatic rebound were high;  
517 Phase 2 around 1180 AD, which is in agreement with a large-scale terrestrial landslide  
518 observed in Quyon Valley (western Québec) dated at  $\sim 1020$  cal. yr BP (Brooks, 2013a); and  
519 Phase 3 corresponding to the well documented CKSZ 1663 AD historical earthquake.  
520 However, aseismic triggers are still considered for the first phase of mass-movement deposits  
521 because deglacial environments were characterized by high sedimentation rates and water  
522 level variation. The  $^{210}\text{Pb}$  analysis revealing a depositional rate of  $0.07 \text{ cm yr}^{-1}$  in Lake St-  
523 Joseph allow us to revise the Normandeau et al (2013) date for a large-scale MMD to the M  
524  $\geq 7$  historical 1663 AD event.

525 Even though the dating represents a minimal age due to errors induced by the sediment

526 compaction and time-traveling-depth variations in the sediments, taken together, our dataset  
527 leads us to conclude that a high magnitude seismic event occurred a few hundred years before  
528 the CKSZ 1663 AD historical earthquake. We observed that a large-scale MMDs event (ME2:  
529 4.09 km<sup>2</sup>, ≤ 7 m thick) recorded in Lake Maskinongé was seismically-induced by the WQSZ  
530  $M \geq 6.3$  earthquake previously reported by Brooks (2013a) and dated at ~ 1020 yr BP.

531 The largest MMDs in the three lakes do not correspond to the same phases (Phase 2 in Lake  
532 Maskinongé vs Phase 3 in Lake Aux-Sables and St-Joseph) suggesting that the seismological  
533 events epicenters occurred at different location (WQSZ vs CKSZ). Although Phase 2 (~ 1020  
534 yr BP) MMDs are more extensive in Lake Maskinongé than those of Phase 3 (1663 AD,  $M > 7$ )  
535 MMDs, the event of Phase 2 was not necessarily of a higher magnitude because the  
536 occurrence of a mass-movement a few hundred years prior to the 1663 AD historical  
537 earthquake must have reduced the sediment availability. Investigations aiming to reconstruct  
538 paleoearthquakes must contextualized MMDs in a regional stratigraphic framework and  
539 consider the recurrence of slope failures. More morphostratigraphic and sediment core data  
540 are needed in eastern Canada to define the extent, exact timing and geomorphological impact  
541 of the events of phases 2 & 3.

542 This study has demonstrated that hydroacoustic investigations coupled with the analysis of  
543 sediment cores in lakes located farther away from an active seismic zone provide a reliable  
544 record of strong earthquakes in a context of frequent lower magnitudes earthquakes and low  
545 sedimentation rates. Different levels of MMDs can be identified in the lakes basin infill, but  
546 these deposits must all be separated by normal sedimentation to deduce their thickness and  
547 depth.

548 The coring data show that RDLs are not necessarily related to seismically-induced  
549 sublacustrine mass-movements, but can be generated by different events occurring in a lake  
550 basin and watershed. Moreover, RDL analysis does not provide information on the  
551 disturbance rate of a lacustrine basin since they might not always be observed in the cores.  
552 Therefore, sediment core data are considered complementary to swath bathymetric imagery  
553 and sub-bottom profiler data and contextualizing them in a morphostratigraphic framework  
554 enhances the detail of paleoseismological reconstructions. Further investigations using a  
555 lower frequency subbottom profiler (e.g., boomer) showing the entire Quaternary  
556 stratigraphic sequence and multiple long sediment cores should be undertaken in these lakes  
557 as well as others of eastern Canada in order to extend the sedimentary archives of mass-  
558 movements.

## 559 **ACKNOWLEDGMENTS**

560 The research was funded by a Discovery grant from the Natural Science and Engineering  
561 Research Council of Canada (NSERC) to P.L. Survey instruments were acquired from  
562 Canadian Foundation for Innovation (CFI) and the Ministère de l'Éducation du Québec. We  
563 thank the *Centre touristique Duchesnay* for their accommodations and the lake access. We  
564 thank François-Xavier L'Heureux-Houde for his assistance during fieldwork and Gabriel  
565 Joyal for his technical and scientific support. Pierre Francus (INRS ETE) and Dermot  
566 Antoniades (U.Laval) provided helpful comments on a previous version of the manuscript.  
567 We also thank G. Brooks (Geological Survey of Canada) and an anonymous reviewer for  
568 providing valuable comments that improved the quality of the manuscript.

569 **REFERENCES CITED**

- 570 Adams, J., Basham P. (1989) The seismicity and seismotectonics of Canada east of the  
571 Cordillera. *Geoscience Canada*, 16 (1): 3-16
- 572 ArchivesCanada: [http://archivescanada.accesstomemory.ca/mastigouche-riviere-dautray-](http://archivescanada.accesstomemory.ca/mastigouche-riviere-dautray-quebec)  
573 [quebec](http://archivescanada.accesstomemory.ca/mastigouche-riviere-dautray-quebec)
- 574 Arnaud, F., Lignier, V., Revel, M., Desmet, M., Beck, C., Pourchet, M., Charlet, F.,  
575 Trentesaux, A., Tribovillard, N. (2002) Flood and earthquake disturbance of 210Pb  
576 geochronology (Lake Anterne, NW Alps). *Terra Nova*, 14: 225-232
- 577 Arnaud, F., Revel, M., Chapron, E., Desmet, M., Tribovillard, N. (2007) 7200 years of  
578 Rhône River flooding activity in Lake Le Bourget, France: a high-resolution sediment  
579 record of NW Alps hydrology. *The Holocene*: 420-428
- 580 Aylsworth, J.M., Lawrence, D.E., Guertin, J. (2000) Did two massive earthquakes in the  
581 Holocene induce widespread landsliding and near-surface deformation in part of the  
582 Ottawa Valley, Canada? *Geology* 28: 903–906
- 583 Beck, C. (2009) Late Quaternary lacustrine paleo-seismic archives in north-western Alps:  
584 Examples of earthquake-origin assessment of sedimentary disturbances. *Earth-Science*  
585 *Reviews*, 96: 327-344
- 586 Beck, C., Manalt, F., Chapron, E., Van Rensbergen, P., De Batist, M. (1996) Enhanced  
587 seismicity in the early post-glacial period: evidence from the post-würm sediments of Lake  
588 Annecy, Northwestern Alps. *Journal of Geodynamics*, 22 (1/2): 155-171

- 589 Bertrand, S., Charlet, F., Chapron, E., Fagel, N., De Batist, M. (2008) Reconstruction of  
590 the Holocene seismotectonic activity of the Southern Andes from seismites recorded in  
591 Lago Icalma, Chile. *Palaeogeography, Palaeoclimatology, Palaeoecology*, 259: 301-322
- 592 Brooks, G.R. (2013a) A massive sensitive clay landslide, Quyon Valley, southwestern  
593 Quebec, Canada, and evidence for a paleoearthquake triggering mechanism. *Quaternary*  
594 *Research*, 80: 425-434.
- 595 Brooks, G.R. (2013b) Prehistoric sensitive clay landslides and paleoseismicity in the  
596 Ottawa Valley, Canada. In *Landslides in sensitive clays: from geosciences to risk*  
597 *management*, L'Heureux, J.-S., Locat, A., Leroueil, S. Demers, D. and Locat, J. (eds.),  
598 *Advances in Natural and Technological Hazards Research 36*, Springer Netherlands,  
599 Dordrecht: 119-131.
- 600 Brooks, G.R. (2015) An integrated stratigraphic approach to investigating evidence of  
601 paleoearthquakes in lake deposits of eastern Canada. *Geoscience Canada*, 42: 247-261.
- 602 Brooks, G. R. (2016) Evidence of late glacial paleoseismicity from submarine landslide  
603 deposits within Lac Dasserat, northwestern Quebec, Canada. *Quaternary Research*, 86 (2):  
604 184-199
- 605 Cauchon-Voyer, G., Locat, J., St-Onge, G. (2008) Late-Quaternary morpho-sedimentology  
606 and submarine mass movements of the Betsiamites area, Lower St. Lawrence estuary,  
607 Quebec, Canada. *Marine Geology*, 251: 233-252
- 608 Chappaz, A., Gobeil, C., Tessier, A. (2008) Sequestration mechanisms and anthropogenic

- 609 inputs of rhenium in sediments from Eastern Canada lakes. *Geochimica et Cosmochimica*  
610 *Acta*, 72: 6027-6036
- 611 Chapron, E., Van Rensbergen, P., Beck, C., De Batist, M., Paillet, A. (1996) Lacustrine  
612 sedimentary records of brutal events in Lake Le Bourget (Northwestern Alps-Southern  
613 Jura). *Quaternaire*, 7 (2-3): 155-168
- 614 Chapron, E., Beck, C., Pourchet, M., Deconinck, J.F. (1999) 1822 earthquake-triggered  
615 homogenite in Lake Le Bourget (NW Alps). *Terra Nova*, 11: 86-92
- 616 Chapron, E., Fain, X., Magand, O., Charlet, L., Debret, M., Mélières, M.A. (2007)  
617 Reconstructing recent environmental changes from proglacial lake sediments in the  
618 Western Alps (Lake Blanc Huez, 2543 m a.s.l., Grandes Rousses Massif, France).  
619 *Palaeogeography, Palaeoclimatology, Palaeoecology*, 252: 586-600
- 620 De Blasio, F.V., Engvik, L., Harbitz, C.B., Elverhøi, A. (2004) Hydroplaning and  
621 submarine debris flows. *Journal of Geophysical Research*, 109: 1-15
- 622 Doig, R. (1986) A method for determining the frequency of large magnitude earthquakes  
623 using lake sediments. *Canadian Journal of Earth Sciences*, 23: 930-937
- 624 Doig, R. (1991) Effects of strong seismic shaking in lake sediments, and earthquake  
625 recurrence interval, Temiscaming, Quebec. *Canadian Journal of Earth Sciences*, 28: 1349-  
626 1352
- 627 Doig, R. (1998) 3000-Year paleoseismological record from the region of the 1988  
628 Saguenay, Quebec, earthquake. *Bulletin of the Seismological Society of America*, 88 (5):

629 1198-1203

630 Doughty, M., Eyles, N., Daurio, L. (2010a). Ongoing neotectonic activity in the  
631 Timiskaming- Kipawa area of Ontario and Québec. *Geoscience Canada* 37(3): 1-8.

632 Doughty, M., Eyles, N. and Daurio, L. (2010b) Earthquake-triggered slumps (1935  
633 Timiskaming M6.2) in Lake Kipawa, Western Quebec Seismic Zone,  
634 Canada. *Sedimentary Geology* 228: 113-118.

635 Doughty, M., Eyles, N., Eyles, C., Talling, P. (2013). High-resolution seismic reflection  
636 profiling of neotectonic faults in Lake Timiskaming, Timiskaming Graben, Ontario-  
637 Quebec, Canada. *Sedimentology* 60(4): 983-1006.

638 Doughty, M., Eyles, N., Eyles, C.H., Wallace, K., Boyce, J.I. (2014) Lake sediments as  
639 natural seismographs: Earthquake-related deformations (seismites) in central Canadian  
640 lakes. *Sedimentary Geology*, 313: 45-67

641 Duboc, Q., St-Onge, G., & Lajeunesse, P. (2017). Sediment records of the influence of  
642 river damming on the dynamics of the Nelson and Churchill Rivers, western Hudson Bay,  
643 Canada, during the last centuries. *The Holocene*, 27(5): 712-725.

644 Duchesne, M.J., Pinet, N., Bédard, K., St-Onge, G., Lajeunesse, P., Calvin Campbell, D.,  
645 Bolduc, A. (2010) Role of the bedrock topography in the Quaternary filling of a giant  
646 estuarine basin : The lower St. Lawrence estuary, Eastern Canada. *Basin Research*, 22:  
647 933-951

648 Fanetti, D., Anselmetti, F.S., Chapron, E., Sturm, M., Vezzoli, L. (2008) Megaturbidite

- 649 deposits in the Holocene basin fill of Lake Coo (Southern Alps, Italy). *Palaeogeography,*  
650 *Palaeoclimatology, Palaeoecology*, 259: 323-340
- 651 Gagné, H., Lajeunesse, P., St-Onge, G., Bolduc, A. (2009) Recent transfert of coastal  
652 sediments to the Laurentian Channel, Lower St. Lawrence Estuary (Eastern Canada),  
653 through submarine canyon and fan system. *Geo-Marine Letters*, 29 (3): 191-200
- 654 Henkel, D.J. (1970) The role of waves in causing submarine landslides. *Geotechnique*, 20:  
655 75-80
- 656 Hilbe, M, Anselmetti, F.S. (2014) Signature of slope failures and river-delta collapses in a  
657 perialpine lake (Lake Lucerne, Switzerland). *Sedimentology*, 61: 1883-1907
- 658 Hilbe, M., Anselmetti, F.S., Eilertsen, R.S., Hansen, L., Wildi, W. (2011) Subaqueous  
659 morphology of Lake Lucerne (Central Switzerland): implications for mass movements and  
660 glacial history. *Swiss Journal of Geosciences*, 104: 425-443
- 661 Lajeunesse, P., & Allard, M. (2002). Sedimentology of an ice-contact glaciomarine fan  
662 complex, Nastapoka Hills, eastern Hudson Bay, northern Québec. *Sedimentary Geology*,  
663 152(3-4) : 201-220.
- 664 Lajeunesse, P., St-Onge, G. (2008) Mouvements de masse subaquatiques postglaciaires au  
665 lac Jacques-Cartier, Réserve faunique des Laurentides. 4<sup>e</sup> conférence canadienne sur les  
666 géorisques : des causes à la gestion. *Presse de l'Université Laval, Québec*: 313-321
- 667 Lajeunesse, P., Sinkunas, B., Morissette, A., Normandeau, A., Joyal, G., St-Onge, G.,  
668 Locat, J. (2017) Large-scale seismically-induced mass-movements in a former glacial lake

- 669 basin: Lake Témiscouata, northeastern Appalachians (eastern Canada). *Marine Geology*,  
670 doi: 10.1016/j.margeo.2016.04.007
- 671 Lamontagne, M. (1987) Seismic activity and structural features in the Charlevoix region,  
672 Quebec. *Canadian Journal of Earth Sciences*, 24: 2118-2129
- 673 Lauterbach, S., Chapron, E., Brauer, A., Hüls, M., Gilli, A., Arnaud, F., Piccin, A., Nomade,  
674 J., Desmet, M., von Grafenstein, U. (2012) A sedimentary record of Holocene surface  
675 runoff events and earthquake activity from Lake Iseo (Southern Alps, Italy). *The Holocene*,  
676 22 (7): 749-760
- 677 Ledoux, G., Lajeunesse, P., Chapron, E., St-Onge, G. (2010) Multibeam Bathymetry  
678 Investigations of Mass Movements in Lake Le Bourget (NW Alps, France) Using a  
679 Portable Platform. *Submarine Mass Movements and Their Consequences, Advances in  
680 Natural and Technological Hazards Research*, 28: 423-434
- 681 Locat, J., Lee, H.J. (2002) Submarine landslides: advances and challenges. *Canadian  
682 Geotechnical Journal*, 39: 193-212
- 683 Locat, J. (2011) La localisation et la magnitude du séisme du 5 février 1663 (Charlevoix)  
684 revues à l'aide des mouvements de terrain. *Canadian Geotechnical Journal*, 48: 1266-1286
- 685 Locat, J., Turmel, D., Habersetzer, M., Trottier, A.P., Lajeunesse, P., St-Onge, G. (2016)  
686 Earthquake Induced Landslides in Lake Éternité, Québec, Canada. *Submarine Mass  
687 Movements and Their Consequences, Advances in Natural and Technological Hazards  
688 Research*, 41: 361-370

- 689 Moernaut, J., De Batist, M. (2011) Frontal emplacement and mobility of sublacustrine  
690 landslides: Results from morphometric and seismostratigraphic analysis. *Marine Geology*,  
691 285: 29-45
- 692 Monecke, K., Anselmetti, F.S., Becker, A., Sturm, M., Giardini, D. (2004) The record of  
693 historic earthquakes in lake sediments of Central Switzerland. *Tectonophysics*, 394: 21-40
- 694 Natural Resources Canada (2018) *Earthquakes Canada*.  
695 <http://www.earthquakescanada.nrcan.gc.ca>
- 696 Nomade, J., Chapron, E., Desmet, M., Reyss, J.L., Arnaud, F., Lignier, V. (2005)  
697 Reconstructing historical seismicity from lake sediments (Lake Laffrey, Western Alps,  
698 France). *Terra Nova*, 17: 350-357
- 699 Normandeau, A., Lajeunesse, P., Philibert, G. (2013) Late-Quaternary morphostratigraphy  
700 of Lake St-Joseph: Evolution from a semi-enclosed glaciomarine basin to a postglacial lake.  
701 *Sedimentary Geology*, 295: 38-52
- 702 Normandeau, A., Lajeunesse, P., Trottier, A-P., G. Poiré, A., Pienitz, R. (2017)  
703 Sedimentation in isolated glaciomarine embayments during glacio-isostatically induced  
704 relative sea level fall (northern Champlain Sea basin). *Canadian Journal of Earth Sciences*,  
705 54(10): 1049-1062
- 706 Occhietti, S. (2007) The Saint-Narcisse morainic complex and early Younger Dryas events  
707 on the southeastern margin of the Laurentide Ice Sheet. *Géographie physique et*  
708 *Quaternaire*, 61: 89-117.

- 709 Occhietti, S., Parent, M., Lajeunesse, P., Robert, F., Govare, E. (2011) Late Pleistocene –  
710 Early Holocene decay of the Laurentide Ice Sheet in Québec-Labrador. In: Ehlers, J.,  
711 Gibbard, P.L. (Eds.), Quaternary Glaciations – Extent and Chronology: Part IV: A closer  
712 look. *Developments in Quaternary Science* 15. Elsevier Science: 601-630.
- 713 Occhietti, S., Richard, P. (2003). Effet réservoir sur les âges <sup>14</sup>C de la Mer de Champlain  
714 à la transition Pléistocène-Holocène: révision de la chronologie de la déglaciation au  
715 Québec méridional. *Géographie physique et Quaternaire*, 57(2-3): 115-138.
- 716 Ouellet, M. (1997) Lake Sediments and Holocene seismic hazard assessment within the St.  
717 Lawrence Valley, Québec. *Geological Society of America Bulletin*, 109 (6): 631-642
- 718 Parent, M., Occhietti, S. (1988) Late Wisconsinan Deglaciation and Champlain Sea  
719 Invasion in the St. Lawrence Valley, Québec. *Géographie physique et Quaternaire*, 42 (3):  
720 215-246
- 721 Père Pierre Gouin (2001) «Historical» earthquakes felt in Québec. Guérin éditeur ltée,  
722 Montreal
- 723 Praet, N., Moernaut, J., Van Daele, M., Boes, E., Haeussler, P.J., Strupler, M., Schmidt, S.,  
724 Loso, M.G., De Batist, M. (2016) Paleoseismic potential of sublacustrine landslide records  
725 in a high-seismicity setting (south-central Alaska). *Marine Geology*, doi:  
726 10.016/j.margeo.2016.05.004
- 727 Schnellmann, M., Anselmetti, F.S., Giardini, D., McKenzie, J.A. (2006) 15.000 Years of  
728 mass-movement history in Lake Lucerne: Implications for seismic and tsunami hazards.

- 729 *Eclogae Geologicae Helvetiae*, 99: 409-428
- 730 Schnellmann, M., Anselmetti, F.S., Giardini, D., McKenzie, J.A., Ward, S.N. (2002)
- 731 Prehistoric earthquake history revealed by lacustrine slump deposits. *Geological Society*
- 732 *of America Bulletin*, 30 (12): 1131-1134
- 733 Shilts, W.W. (1984) Sonar evidence for postglacial tectonic instability of the Canadian
- 734 Shield and Appalachians. *Current Research, Part A, Geological Survey of Canada*: 567-
- 735 579
- 736 Shilts, W.W., Rappol, M., Blais, A. (1992) Evidence of late and postglacial seismic activity
- 737 in the Temiscouata-Madawaska valley, Quebec-New Brunswick, Canada. *Canadian*
- 738 *Journal of Earth Sciences*, 29: 1043-1069
- 739 Shilts, W.W., Clague, J.J. (1992) Documentation of earthquake-induced disturbance of
- 740 lake sediments using subbottom acoustic profiling. *Canadian Journal of Earth Sciences*,
- 741 29: 1018-1042
- 742 Sims, J.D. (1975) Determining earthquake recurrence intervals from deformational
- 743 structures in young lacustrine sediments. *Tectonophysics*, 29: 141-152
- 744 Smith, S.B., Karlin, R.E., Kent, G.M., Seitz, G.G., Driscoll, N.W. (2013) Holocene
- 745 subaqueous paleoseismology of Lake Tahoe. *Geological Society of America Bulletin*, 125
- 746 (5/6): 691-708

- 747 St-Onge, G., Mulder, T., Piper, D. J., Hillaire-Marcel, C., & Stoner, J. S. (2004).  
748 Earthquake and flood-induced turbidites in the Saguenay Fjord (Québec): a Holocene  
749 paleoseismicity record. *Quaternary Science Reviews*, 23(3): 283-294.
- 750 St-Onge, G., Chapron, E., Mulsow, S., Salas, M., Viel, M., Debret, M., ... & Costa, P. J.  
751 (2012). Comparison of earthquake-triggered turbidites from the Saguenay (Eastern  
752 Canada) and Reloncavi (Chilean margin) Fjords: Implications for paleoseismicity and  
753 sedimentology. *Sedimentary Geology*, 243: 89-107.
- 754 Strasser, M., Anselmetti, F.S., Fäh, D., Giardini, D., Schnellmann, M. (2006) Magnitudes  
755 and source areas of large prehistoric northern Alpine earthquakes revealed by slope failures  
756 in lake. *Geological Society of America Bulletin*, 34 (12): 1005-1008
- 757 Strasser, M., Hilbe, M., Anselmetti, F.S. (2011) Mapping basin-wide subaquatic slope  
758 failure susceptibility as a tool to assess regional seismic and tsunami hazards. *Marine*  
759 *Geophysical Research*, 32: 331-347
- 760 Tremblay, A., Roden-Tice, M. K., Brandt, J. A., Megan, T. W. (2013). Mesozoic fault  
761 reactivation along the St. Lawrence rift system, eastern Canada: Thermochronologic  
762 evidence from apatite fission-track dating. *Geological Society of America Bulletin* 125(5-  
763 6): 794-810.
- 764 Tuttle, M., Atkinson, G.M. (2010) Localization of large earthquakes in the Charlevoix  
765 seismic zone, Quebec, Canada, during the past 10 000 years. *Seismological Research*  
766 *Letters*, 81 (1): 140-147

767 Wilhelm, B., Nomade, J., Crouzet, C., Litty, C., Sabatier, P., Belle, S., Anselmetti, F. S.  
768 (2016). Quantified sensitivity of small lake sediments to record historic earthquakes:  
769 Implications for paleoseismology. *Journal of Geophysical Research: Earth Surface*, 121(1):  
770 2-16.

771 **Table of figures**

772 Figure 1 – A) Seismic hazard potential in Canada (modified from NRCan); B) Location  
773 map of the investigated lakes north of the St. Lawrence River within the deglacial  
774 Champlain Sea limit and between two active seismic zones: the Western Québec seismic  
775 zone (WQSZ) and the Charlevoix-Kamouraska seismic zone (CKSZ).

776 Figure 2 – Morphologies and facies associated with sublacustrine mass-movements as  
777 observed on the hydroacoustic data of the investigated lakes.

778 Figure 3 - General stratigraphic framework observed on the acoustic sub-bottom profiles  
779 of the investigated lakes summarizing the units (U1 to U7) previously identified by  
780 Normandeau et al. (2013, 2017): Ua till or bedrock; Ub glaciomarine Champlain Sea  
781 deposits; and Uc paraglacial and postglacial units.

782 Figure 4 – A) High-resolution swath bathymetric imagery of Lake Maskinongé with  
783 location of acoustic sub-bottom profiles and coring site; B) Geomorphological map of the  
784 lake showing disturbed basin morphologies: a wide MMD, headwall scarps and  
785 undisturbed mounds. Linear to sinuous features are also visible at the Mastigouche River  
786 mouth.

787 Figure 5 – Acoustic sub-bottom profiles (12 kHz) of Lake Maskinongé showing the  
788 glaciomarine (Ub) and the paraglacial and postglacial (Uc) sediments. MMDs facies are  
789 observed along three different stratigraphic levels: Event ME1 buried in Ub and Events  
790 ME2 & ME3 in Uc. Note that the uppermost MMD facies (ME3) is only visible on profile  
791 C at a depth of 0.5-1.0 m.

792 Figure 6 – 3D view of the high-resolution swath bathymetric imagery of Lake Maskinongé  
793 coupled with an acoustic profile. The hummocky topography observed on the basin floor  
794 correlate with the extent of the deposit of event ME2, suggesting that the disturbed  
795 morphology of Lake Maskinongé was caused by the second phase of mass-movement.

796 Figure 7 – Photography, CT-Scan image, CT-number, magnetic susceptibility and location  
797 on acoustic sub-bottom profiles of the cores sampled in Lake Maskinongé (MAS15-1aP),  
798 Aux-Sables (LAS15-1P) and St-Joseph (LSJ15-1bP). Layers of high CT-number and  
799 magnetic susceptibility values are visible on the upper section of the cores and their date  
800 of deposition were inferred from each lake respective sedimentation rate.

801 Figure 8 –  $^{210}\text{Pb}$  (A) and  $^{137}\text{Cs}$  (B) radiometric activity of the studied lakes. The slopes  
802 resulting from  $\ln(^{210}\text{Pb excess})$  vs depth indicate depositional rates of  $0.18 \text{ cm yr}^{-1}$  for Lake  
803 Maskinongé,  $0.08 \text{ cm yr}^{-1}$  for Lake Aux-Sables and  $0.07 \text{ cm yr}^{-1}$  for Lake St-Joseph.

804 Figure 9 – A) High-resolution swath bathymetric imagery of Lake Aux-Sables with  
805 location of acoustic sub-bottom profiles and coring site; B) Geomorphological map of the  
806 lake showing disturbed basin morphologies: wide MMDs and numerous headwall scarps.

807 Figure 10 –3D view of the high-resolution swath bathymetric imagery of Lake Aux-Sables  
808 showing the direction of flow of mass-movements and the extent of their deposits on the  
809 basin floor.

810 Figure 11 – Acoustic sub-bottom profiles (3.5 kHz) of Lake Aux-Sables showing the ice-  
811 contact (Ua), the glaciomarine (Ub) and the paraglacial and postglacial (Uc) sediments.  
812 Recent MMDs facies are observed in Uc on both profiles.

813 Figure 12 – A) High-resolution swath bathymetric imagery of Lake St-Joseph with location  
814 of acoustic sub-bottom profiles and coring site; B) Geomorphological map of the lake  
815 showing disturbed basin morphologies: wide MMD, headwall scarps, an undisturbed  
816 mound and compression ridges.

817 Figure 13 –3D view of the high-resolution swath bathymetric imagery of Lake St-Joseph  
818 showing the direction of flow of mass-movement and the extent of its deposit. Compression  
819 ridges are visible in zone of frontal thrusting.

820 Figure 14 – Acoustic sub-bottom profiles (12 kHz) of Lake St-Joseph showing the ice-  
821 contact (Ua), the glaciomarine (Ub) and the paraglacial and postglacial (Uc) sediments.  
822 MMDs facies are observed along three different stratigraphic levels: Events JE1 and JE2  
823 buried in Ub and Event JE3 in Uc.

**Table 1**

Physical characteristics of the investigated lakes.

Lake	Coordinates	Elevation (m) asl	Distance from WQSZ *(km)	Distance from CKSZ *(km)	Maximum depth (m)	Area (km <sup>2</sup> )
Maskinongé	46°19.78N 73°23.92W	140	140	285	25	10.2
Aux-Sables	46°52.93N 72°21.95W	150	235	185	41	5.2
St-Joseph	46°55.00N 71°39.00W	160	290	135	37	11.3

\* Distances were measured from the center of the seismic zones to the center of each respective lake.

**Table 2**

Description and location of cores collected in the investigated lakes.

<b>Core number</b>	<b>Lake</b>	<b>Coordinates</b>	<b>Depth (m)</b>	<b>Length (cm)</b>
MAS15-1aP	Maskinongé	46°18.73N 73°23.43W	18.5	105
LAS15-1P	Aux-Sables	46°53.12N 72°22.00W	39	131
LSJ15-1bP	St-Joseph	46°54.82N 71°38.76W	37	123

**Table 3**

Depth, thickness and date of the layers observed in each core.

<b>Core number</b>	<b>Layer</b>	<b>Depth (cm)</b>	<b>Thickness (cm)</b>	<b>Depositional rate (cm yr<sup>-1</sup>)</b>	<b>Calendar age (AD)</b>
MAS15-1aP	ML1	8.5	3.0	0.18	1969
LAS15-1P	SL1	5.5	4.5	0.08	1947
LAS15-1P	SL2	23	3.5	0.08	1785
LAS15-1P	SL3	35	6.0	0.08	1704
LSJ15-1bP	JL1	19	3.5	0.07	1745
LSJ15-1bP	JL2	49	1.0	0.07	1366

**Table 4**

Summarize of the three phases of mass-movements with their respective deposits, date and seismic trigger event.

<b>Phase</b>	<b>MMDs event</b>	<b>Depth (m)</b>	<b>Maximal thickness (m)</b>	<b>Calculated calendar age* (AD)</b>	<b>Seismic event</b>	<b>Seismic zone</b>
	ME1	5.5 - 6.0	-			
1	JE1	> 5.5	4	Deglacial Champlain Sea transgression	11.1 to 10.5 Ka yr BP	-
	JE2	5.5	3			
2	ME2	1.5	7	1180	~ 1020 yr BP	WQSZ
	ME3	0.5 - 1.0	1.5	1739		
3	SE1	-	5	-	1663 AD	CKSZ
	JE3	0.5 – 1.0	10	1685		

\*Note that the calculated age represent a minimal age.

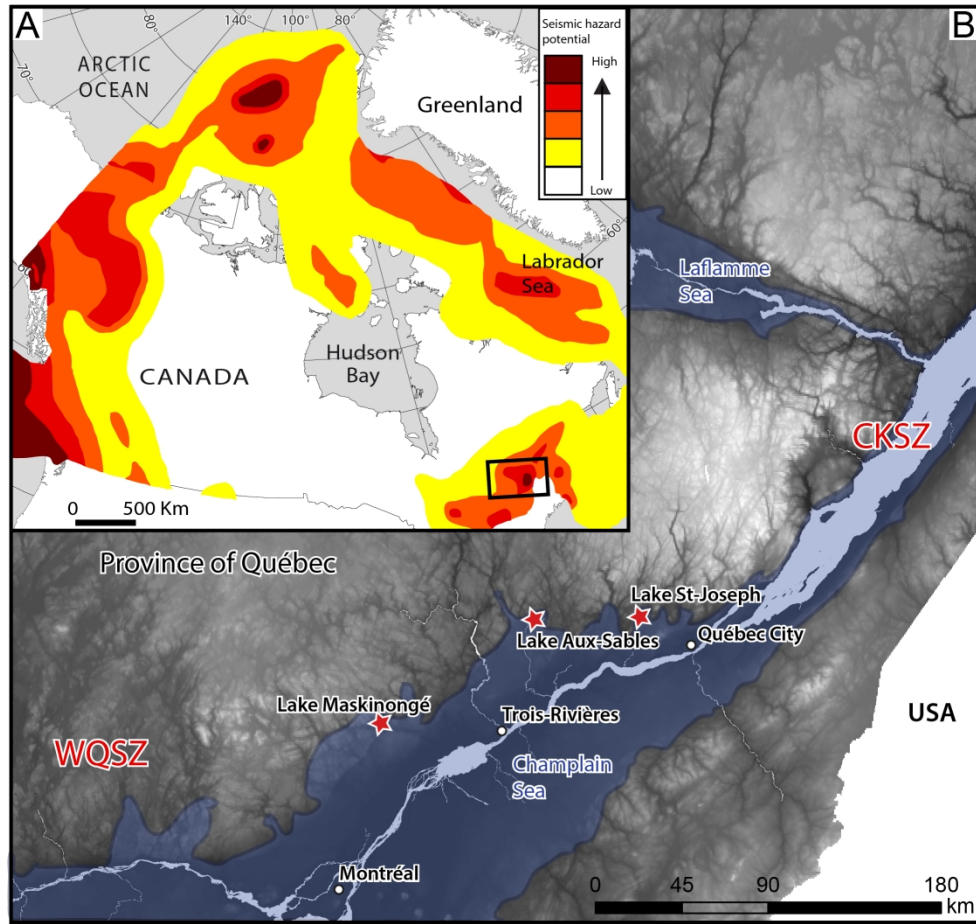


Figure 1 – A) Seismic hazard potential in Canada (modified from NRCan); B) Location map of the investigated lakes north of the St. Lawrence River within the deglacial Champlain Sea limit and between two active seismic zones: the Western Québec seismic zone (WQSZ) and the Charlevoix-Kamouraska seismic zone (CKSZ).

193x183mm (300 x 300 DPI)

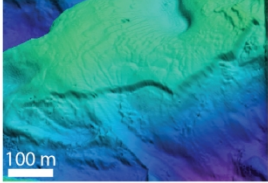
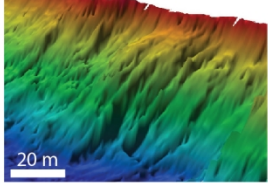
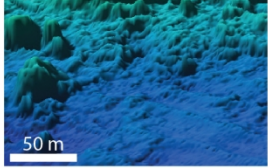
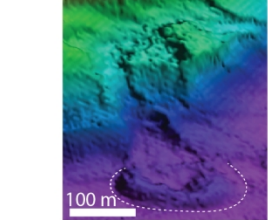
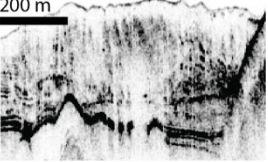
<b>Morphologies</b>	<b>Descriptions</b>	<b>Images on the hydro-acoustic data</b>
<b>Headscarp</b>	Sharp straight line at the slope breaks.	
<b>Gullies</b>	Parallel incisions eroded on lateral slopes.	
<b>Hummocky topography</b>	Chaotic topography in unconformity with the flat basin floors.	
<b>Lobe of hummocky debris</b>	Chaotic topography with an arcuate cambered shape at its front.	
<b>MMDs facies</b>	Acoustically transparent or semi-transparent, with a hummocky topography.	

Figure 2 – Morphologies and facies associated with sublacustrine mass-movements as observed on the hydro-acoustic data of the investigated lakes.

175x210mm (300 x 300 DPI)

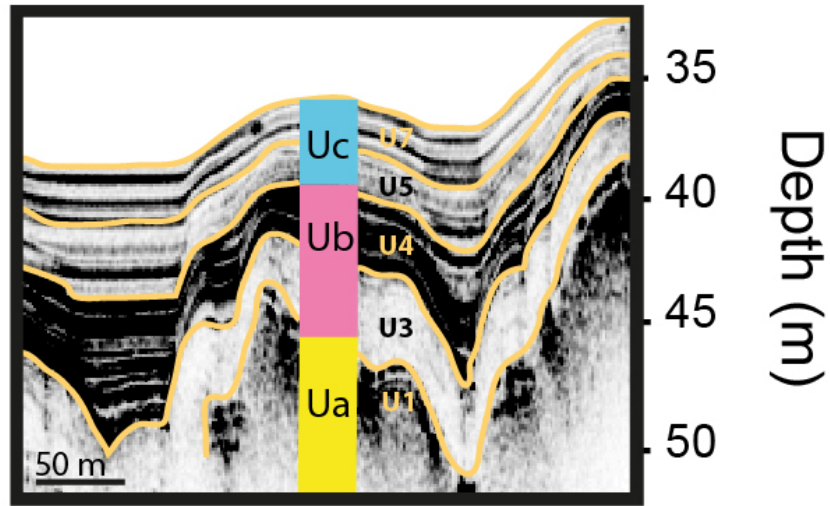


Figure 3 – General stratigraphic framework observed on the acoustic sub-bottom profiles of the investigated lakes summarizing the units (U1 to U7) previously identified by Normandeau et al. (2013, 2017): Ua till or bedrock; Ub glaciomarine Champlain Sea deposits; and Uc paraglacial and postglacial units.

60x40mm (300 x 300 DPI)

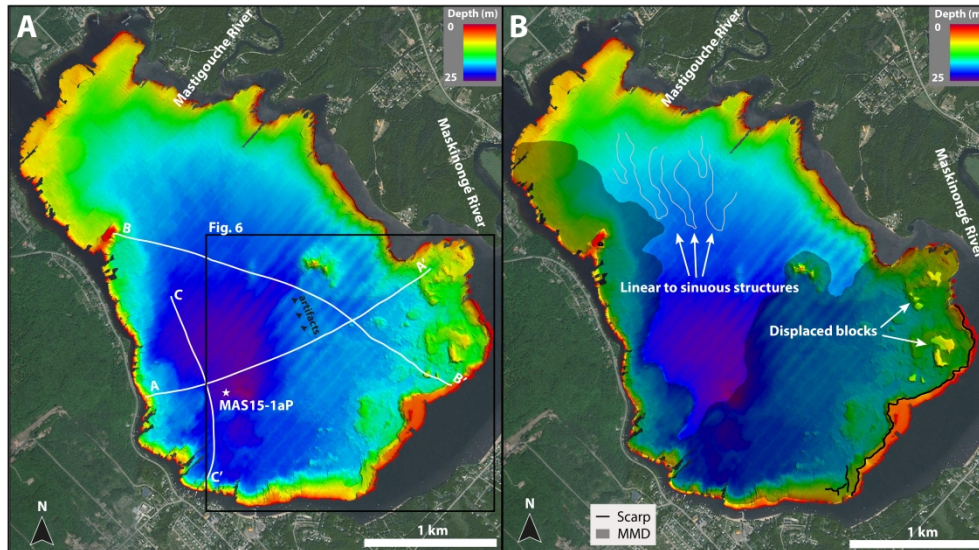


Figure 4 – A) High-resolution swath bathymetric imagery of Lake Maskinongé with location of acoustic sub-bottom profiles and coring site; B) Geomorphological map of the lake showing disturbed basin morphologies: a wide MMD, headwall scarps and undisturbed mounds. Linear to sinuous features are also visible at the Mastigouche River mouth.

437x246mm (300 x 300 DPI)

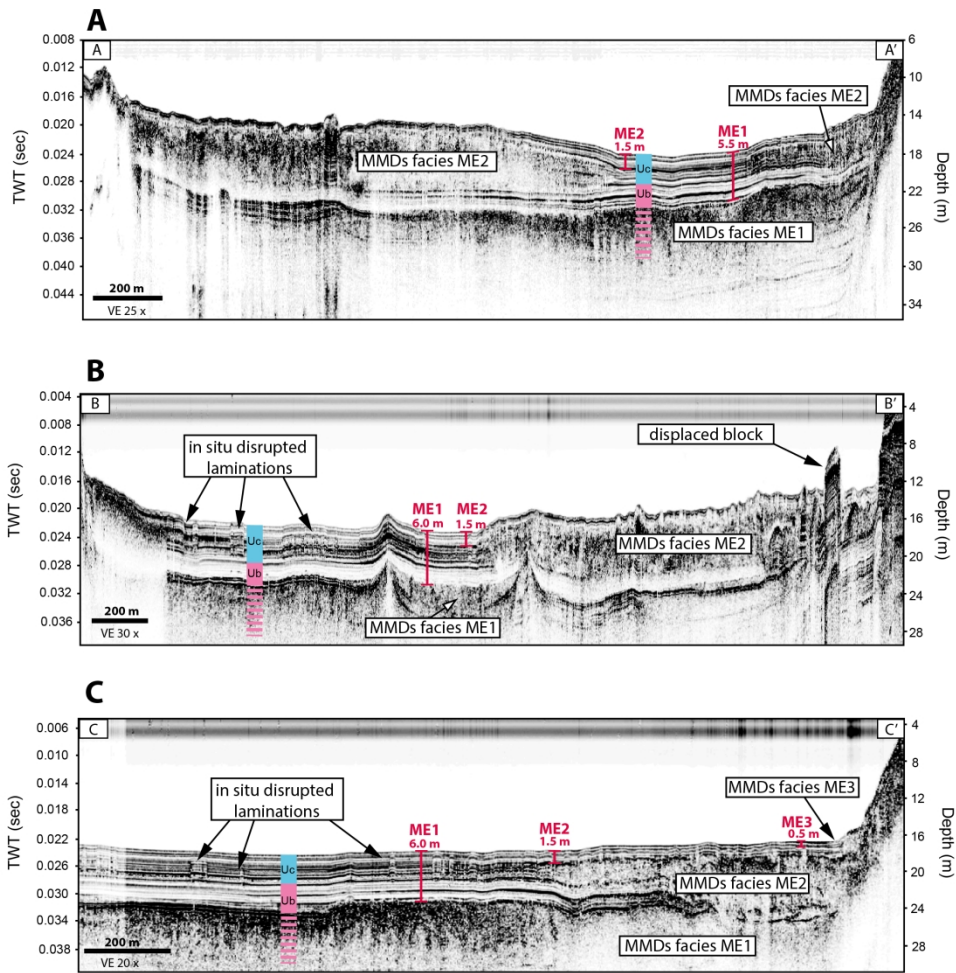


Figure 5 – Acoustic sub-bottom profiles (12 kHz) of Lake Maskinongé showing the glaciomarine (Ub) and the paraglacial and postglacial (Uc) sediments. MMDs facies are observed along three different stratigraphic levels: Event ME1 buried in Ub and Events ME2 & ME3 in Uc. Note that the uppermost MMD facies (ME3) is only visible on profile C at a depth of 0.5-1.0 m.

220x220mm (300 x 300 DPI)

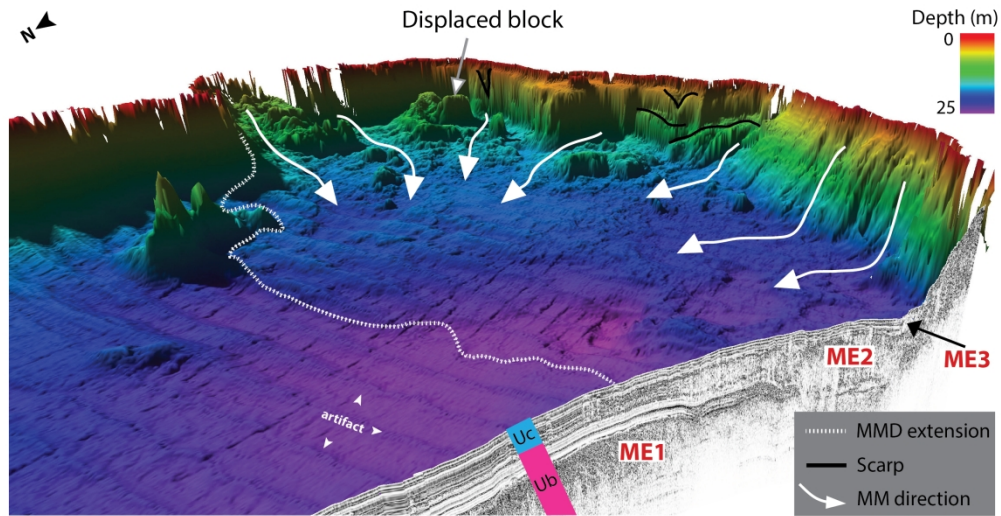


Figure 6 – 3D view of the high-resolution swath bathymetric imagery of Lake Maskinongé coupled with an acoustic profile. The hummocky topography observed on the basin floor correlate with the extent of the deposit of event ME2, suggesting that the disturbed morphology of Lake Maskinongé was caused by the second phase of mass-movement.

258x135mm (300 x 300 DPI)

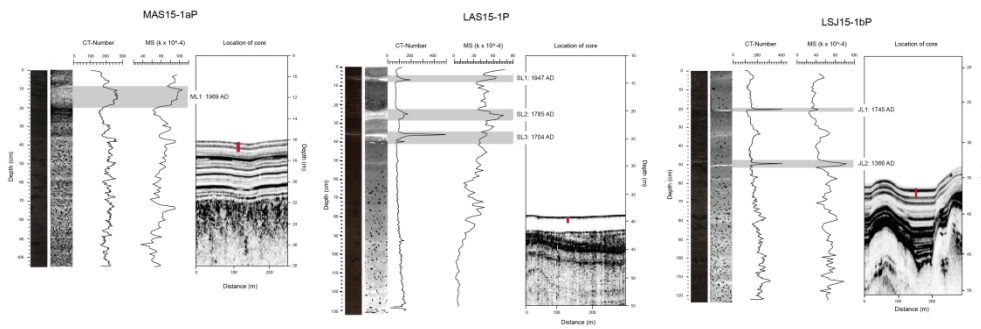
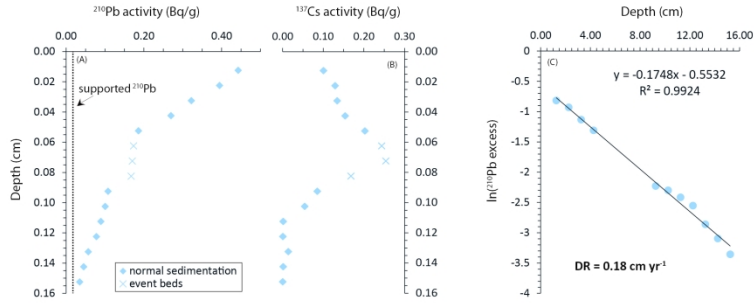


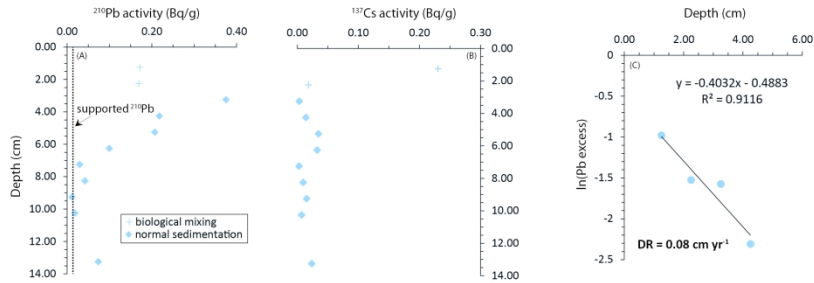
Figure 7 – Photography, CT-Scan image, CT-number, magnetic susceptibility and location on acoustic sub-bottom profiles of the cores sampled in Lake Maskinongé (MAS15-1aP), Aux-Sables (LAS15-1P) and St-Joseph (LSJ15-1bP). Layers of high CT-number and magnetic susceptibility values are visible on the upper section of the cores and their date of deposition were inferred from each lake respective sedimentation rate.

348x123mm (300 x 300 DPI)

### LAKE MASKINONGÉ



### LAKE-AUX-SABLES



### LAKE ST-JOSEPH

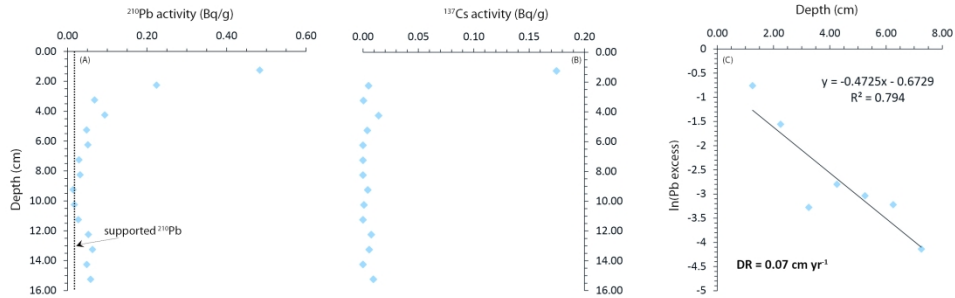


Figure 8 –  $^{210}\text{Pb}$  (A) and  $^{137}\text{Cs}$  (B) radiometric activity of the studied lakes. The slopes resulting from  $\ln(^{210}\text{Pb excess})$  vs depth indicate depositional rates of  $0.18 \text{ cm yr}^{-1}$  for Lake Maskinongé,  $0.08 \text{ cm yr}^{-1}$  for Lake Aux-Sables and  $0.07 \text{ cm yr}^{-1}$  for Lake St-Joseph.

265x292mm (300 x 300 DPI)

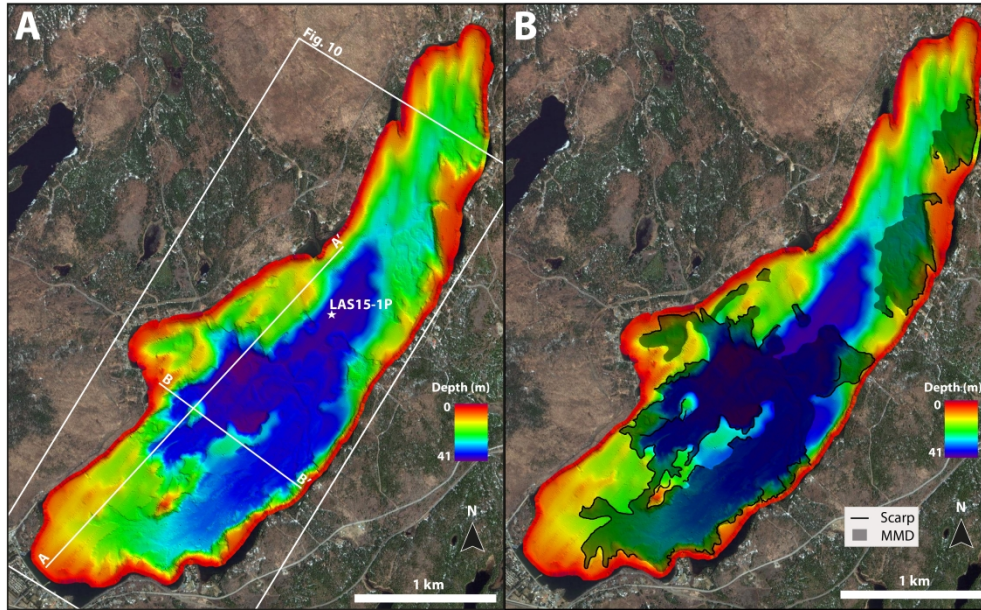


Figure 9 – A) High-resolution swath bathymetric imagery of Lake Aux-Sables with location of acoustic sub-bottom profiles and coring site; B) Geomorphological map of the lake showing disturbed basin morphologies: wide MMDs and numerous headwall scarps.

431x268mm (300 x 300 DPI)

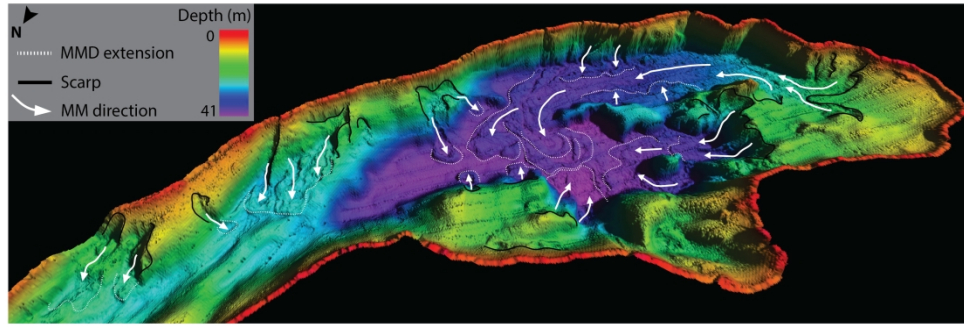


Figure 10 –3D view of the high-resolution swath bathymetric imagery of Lake Aux-Sables showing the direction of flow of mass-movements and the extent of their deposits on the basin floor.

303x104mm (300 x 300 DPI)

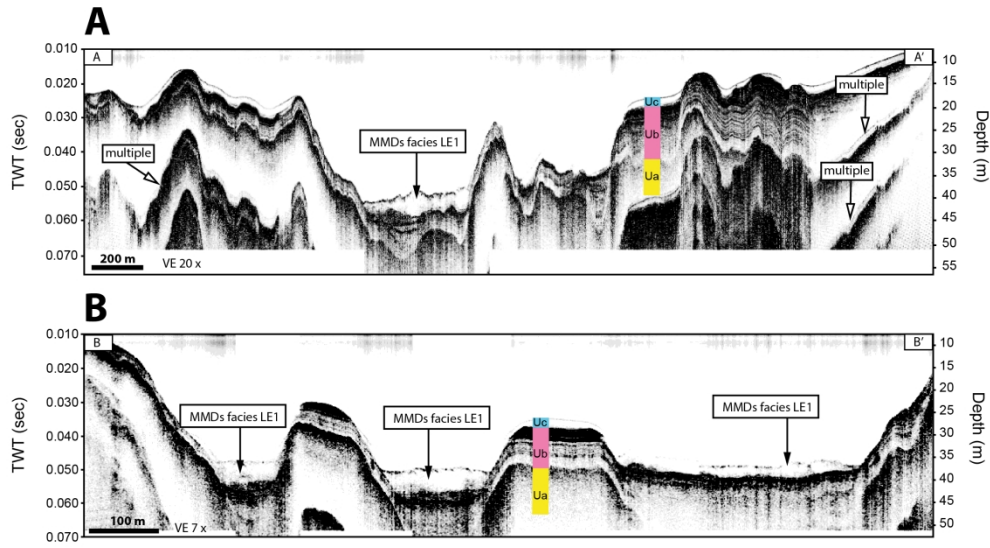


Figure 11 – Acoustic sub-bottom profiles (3.5 kHz) of Lake Aux-Sables showing the ice-contact (Ua), the glaciomarine (Ub) and the paraglacial and postglacial (Uc) sediments. Recent MMDs facies are observed in Uc on both profiles.

216x119mm (300 x 300 DPI)

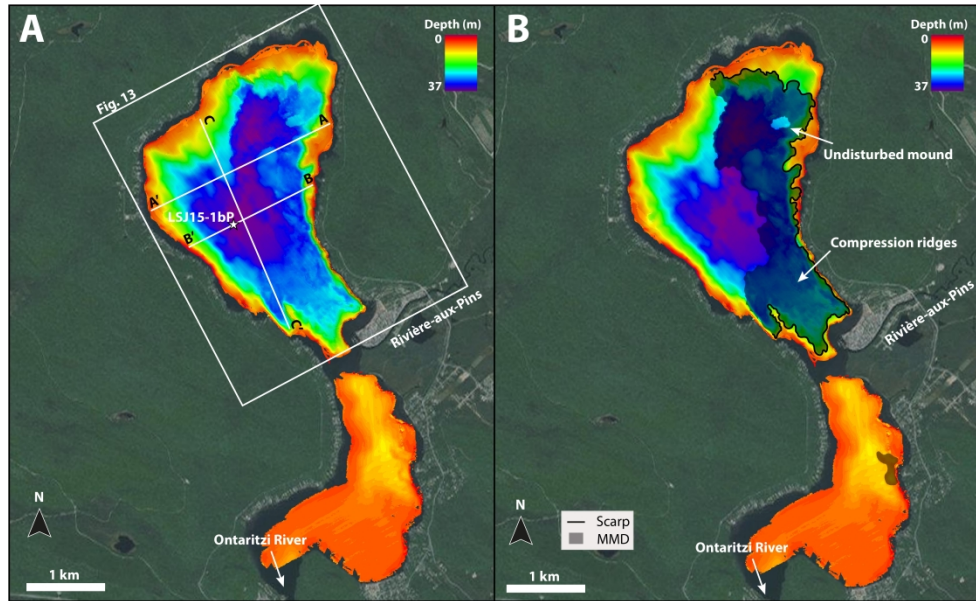


Figure 12 – A) High-resolution swath bathymetric imagery of Lake St-Joseph with location of acoustic sub-bottom profiles and coring site; B) Geomorphological map of the lake showing disturbed basin morphologies: wide MMD, headwall scarps, an undisturbed mound and compression ridges.

440x272mm (300 x 300 DPI)

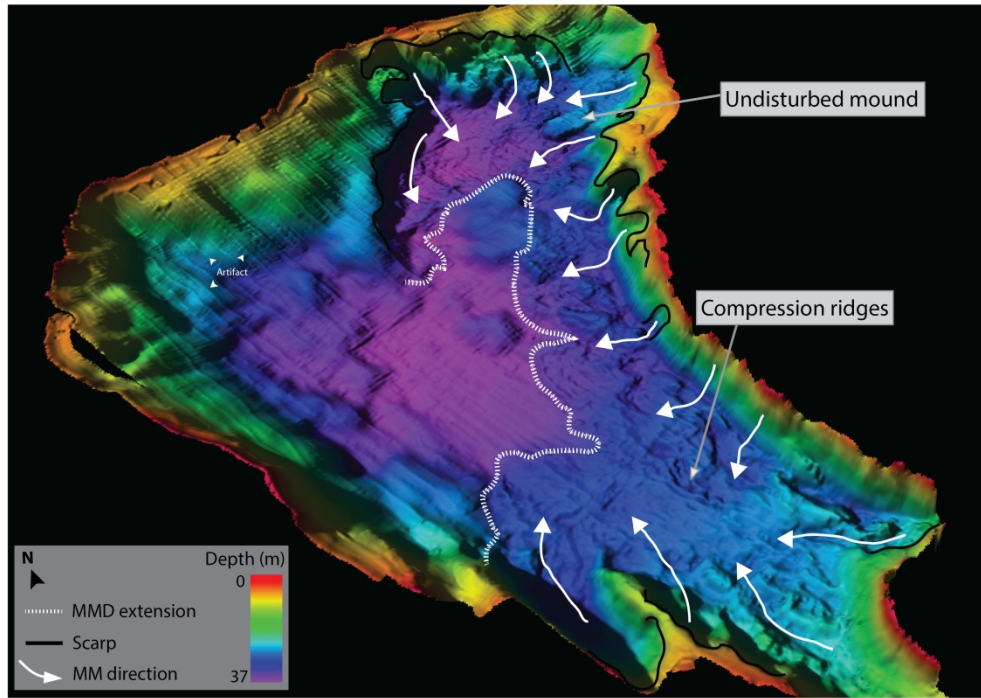


Figure 13 –3D view of the high-resolution swath bathymetric imagery of Lake St-Joseph showing the direction of flow of mass-movement and the extent of its deposit. Compression ridges are visible in zone of frontal thrusting.

279x199mm (300 x 300 DPI)

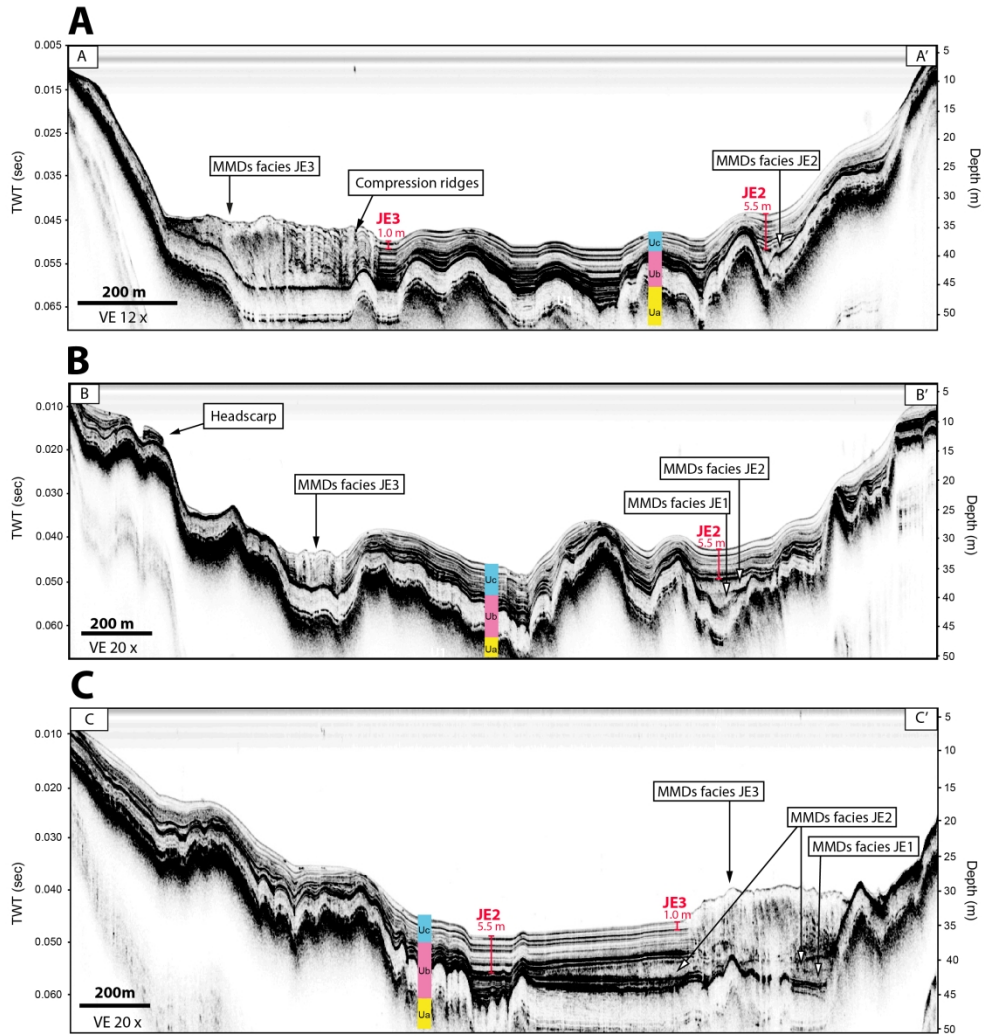


Figure 14 – Acoustic sub-bottom profiles (12 kHz) of Lake St-Joseph showing the ice-contact (Ua), the glaciomarine (Ub) and the paraglacial and postglacial (Uc) sediments. MMDs facies are observed along three different stratigraphic levels: Events JE1 and JE2 buried in Ub and Event JE3 in Uc.

259x278mm (300 x 300 DPI)